A ROCKET DRIVE

FOR

LONG RANGE BOMBERS

(Über einen Raketenantrieb für Fernbomber)

by

E. Sänger and J. Bredt

Ainring, August 1944

Deutsche Luftfahrtforschung

UM 3538

C- 84296

A Note by the Publisher

Toward the end of the last century a few farsighted individuals became thoroughly convinced that man could fly. Today their names are all but forgotten but their technical achievements will endure for centuries.

Today we are on the threshold of manned flight between the planets. Drs. Eugen Sänger and Irene Bredt are prominent among the handful of pioneers whose dedicated efforts have made possible this vista.

"Uber einen Raketenantrieb fur Fernbomber" is based on more than a decade of effort by the authors. The material is condensed. This report contains only about one-third of the information which the authors had available at the time of writing; all of the mathematical derivations and much of the supporting and supplementary information were omitted.

In spite of this fact, the report is, in effect, a definitive treatise. It catalogs new problems and outlines solutions to the more important ones. For years to come it will serve as a storehouse of vital concepts for the serious student of rocket science. For these reasons, its publication at this time seems warranted.

Since 1945, Dr. Irene Bredt (now Sänger-Bredt) and Dr. Eugen Sänger have lived in Paris, where they are employed by the Arsenal de l'Aeronautique. Dr. Sänger is also president of the International Astronautical Federation.

While the Technical Information Branch, BUAER, Navy Department, has very generously furnished copies of their translation of "Uber einen Raketenantrieb fur Fernbomber" to many public libraries and research institutions, this is the first time the report has been available for public sale. The publisher would like to thank the U. S. Navy, without whose permission this publication would not have been possible.

Robert Cornog
Santa Barbara, California
16 November 1952

FOREWORD

The application of pure rocket propulsion to aeronautics suffers at present from limitations imposed on exhaust speed and flight velocity by constructional difficulties.

Because of the thermal stresses on the engines, the exhaust speed is not raised to the physically possible limits.

Because of the mechanical stresses on the airframe, the velocity of flight has not yet gone beyond the velocity of sound.

On the basis of extensive physical and physico-chemical studies, we shall discuss some possibilities which are opened for the rocket propulsion of long-range military aircraft when these two limits are surpassed.

In addition several suggestions as to construction are made, which should facilitate overcoming the present limitations.

These investigations on the problem of long-range military rocket aircraft originated as a joint work of the two authors during the years 1937-1941 and were intended, together with the material of report UM-3509, to be a second volume of "Rocket Flight Technique", by the senior author.

As a result of circumstances caused by the war, publication was postponed and the results of the work issued in abstract form in the present report.

Sänger

(sig.)

Bredt

Ainring (Upper Bavaria), August 1944

TABLE OF CONTENTS

C-84296

I. Fundamentals

The range of flight-speeds several times the velocity of sound is the exclusive province of the pure rocket, which develops the propulsive jet entirely from the fuel carried on board the aircraft. The pure rocket can also compete in cost at lower speeds, if propulsive forces of great magnitude or short duration are required, or if no surrounding air is available, e.g. under water or outside the perceptible atmosphere of the earth. These special characteristics give rocket propulsion a broad domain of application to military techniques, which can be outlined as follows:

Propulsion of projectiles or bombs, in which the relatively strong, short duration propulsive forces can be achieved in most cases by powder-rockets.

Auxiliary drive for propeller-, or jet-aircraft, with operating periods generally under a minute, for which liquid rockets with compression-drive can be used.

Auxiliary or principal propulsion for vessels with period of operation of several minutes, so that rocket motors having fuel pumps, but without high exhaust speed, are required.

Main drive of aerial torpedoes against land, sea, or air targets, with moderate to long times of operation, in which high exhaust speeds are important only for quite large ranges.

Main drive of fighter or bomber aircraft, e.g. for fighter defense at very high altitudes or for military aircraft operating over very great distances. Both propulsion-time and exhaust speed set extreme requirements for the rocket motor. The last-mentioned application, the rocket bomber, is treated in more detail in the present report.

Pure-rocket engines make only very incomplete use of the energy made available by the fuel. However since the craft is not loaded down by the energy carried on board but rather by the weight of the fuel, this disadvantage can be counteracted by use of fuels with the maximum possible energy content per unit weight. Thus rocket fuels represent, on the one hand, carriers of energy with maximum concentration of energy per unit mass and per unit tank space; on the other hand, they are the carriers of those masses from which the jet of the engine is developed.

According to the method of feeding the fuel (which, in the tank, is liquid or solid) into the combustion chamber of the rocket, we can distinguish between various modes of operation of the rocket motor; e.g. rockets with periodic propulsion, which are characterized by moderate values of the work for feeding the fuel, the temperature stresses in the walls in contact with the flame, the exhaust speed and the thrust; and rockets with continuous propulsion, with arbitrarily high constant flame-pressures, high constant exhaust speed, maximum thrust for given dimensions and maximum thermal stresses of the furnace walls.

The type of construction of the walls in contact with the flame is determined by these stresses.

The type of construction using the heat capacity of the wall-material gives very simple solutions, which are however applicable only to periodic propulsion, or to continuous propulsion over short periods at moderate furnace temperatures. For example, the 20 mm. thick metal wall of the jet-throat of a powder-rocket at 2800°K and having thermal conductivity 4000 k cal/m^2h°, begins to melt on the side in contact with the flame after 2, 4, 8, 10, 14 or 90 sec, if it is made of Al, Ag, Cu, Fe or Ni, Pt, or Ir, resp; this can be shown by calculation and can be qualitatively checked by tests on welding torches.

Designs of combustion chamber walls using the best refractory materials give somewhat more complicated arrangements and longer propulsion times, which are in general limited mainly by chemical changes in the wall material. The best heat resistant materials, (melting points given in °C) which would be of interest in this connection are for example: beryllium oxide (2500), molybdenum (2600), zirconium oxide (2700), magnesium oxide (2800), thorium oxide (3050), titanium carbide (3140), rhenium (3170), tungsten (3380), zirconium carbide (3500), tantalum and hafnium carbide (3700) and graphite (4000). With these materials, using non-stationary thermal conditions, the driving times can be extended further than the values given previously.

Design using condenser jackets around the combustion-chamber walls is similar to that used in internal combustion engines for controlling the hot, strongly superheated combustion gases; it is however limited to moderate combustion temperatures and pressures for which the heat flow through the wall is everywhere less than 1 h.p/cm^2 so that the velocity of the coolant need not be raised above about 10 m/sec.

$$l = 4.5 \frac{BTU}{in^2 \, sec}$$

4

Fire-wall construction using forced circulation of the refrigerant in channels, of preferably one-dimensional extent, which cover practically without gaps all the wall surfaces touched by the flame, gives the possibility of controlling also those high heat transfers through the chamber walls which occur unavoidably in using high-grade rocket fuels in uniform-pressure rockets, and which go far above 1 h.p/$_{cm}$2, and can be even 10 h.p/$_{cm}$2 or more in the jet throat. This type of firewall for rocket motor construction is used in the designs of the present work.

Aside from design of firewalls, the supply of fuel to the combustion chamber is, for uniform-pressure rockets, a special problem for the solution of which various methods have been used.

Placing the whole fuel supply in the combustion chamber has proved suitable in short-period powder rockets. Pressure tank feed of liquid fuel, because of the considerable weights of the tanks and compressed air, is possible only for moderate driving periods and fire gas pressures. Fuel supply through gas-pressure pumps limits the tank size and gives longer driving periods at moderate flame pressures. Fuel supply with ordinary pumps and turbine drive require special propellants or exhaust gas removal from the combustion chamber and results in increased fuel requirement per unit momentum; nevertheless, it does give high driving periods and flame pressures. Fuel supply with ordinary pumps using a turbine driven by steam from the refrigerant, where the steam for the turbine is developed by vaporizing the coolant in the canals of the chamber walls and fire-jet, limits neither driving period, driving pressure, or flame temperature, and permits the use of the greatest exhaust speeds. This method is the basis of the rocket motors described here.

Finally, one of the most essential construction problems for uniform pressure rocket motors is the choice of furnace pressure. The high-pressure rockets with furnace pressures above 50 atm. (which are necessary because of the high exhaust speeds required), are in practise driven up to 100 atm. They have small dimensions per unit thrust and are especially valuable combined with highest grade fuels, where the already high exhaust velocity can be increased by 22% through a furnace pressure increase from 10 to 100 atm., and by 6% through a change from 50 to 100 atm. Its domain of application is therefore especially that of rocket flight, e.g. for rocket bombers, where the requirement of high exhaust speed is most stringent. The high requirements on the fuel feed system are no trouble when they are taken care of by the coolant-steam turbine mentioned above, which uses the heat from the forced cooling of the furnace. As a result of increased gas-density,-velocity,-temperature, and - radiation, the specific heatflow from the flame through the furnace walls rises proportionally with the furnace pressure. This has as consequence the decisive difficulty that the protection of the walls in contact with the flame becomes more critical as the furnace pressure increases, since the heat transfer from furnace wall to coolant only increases as the 0.4 power of the coolant pressure, so that a practical limit of furnace pressure is reached at about 100 atm.

Similar general considerations apply to the air-frame. To the fundamental question, whether explosive propulsion by rockets over large distances shall be used with wingless, unmanned rocket-torpedos or with winged and man carrying rocket aircraft, it may be said that for the "returning" aircraft, the range of use and the total destructive energy brought to the target (weight of bomb $\times$ energy of explosive) is as large as for the rocket torpedo for equal initial flight speed, so that the conserving of the empty craft for repeated use and the probably greater bombing accuracy speak in favor of the aircraft. Since the initial cost of the empty craft is far greater than that for the bomb and fuel load, this is the basis for the choice. If the rocket bomber doesn't return to its place of takeoff, its range for equal v_o will be much greater than that of the rocket torpedo, though, of course, the % weight of destructive energy brought to the target decreases. The extreme ranges possible with the rocket bomber are completely forbidden to the rocket torpedo.

The rocket bomber will differ from the present-day propeller-driven bombing aircraft in the following essential points: in place of the propeller propulsion from the fuselage front it has the rocket propulsion in the fuselage stern; the fuselage is in the shape of a bullet with tapered hind part, the wings have a thin wedge-shaped profile with sharp leading and trailing edges and high wing loading at the start of the flight; the cabin is constructed as an airtight stratosphere chamber.

For starting, the use of its own fuel as in the usual propeller-driven aircraft was considered. Because of the great difference in start- and landing-weight this leads to large wing surfaces and too high fuel consumption in the range of speeds below the velocity of sound. Vertical start under its own power has only the last disadvantage, but even in a greater degree. Sling-starting on a horizontal take-off path until the sound velocity is reached appears most favorable and is assumed here. In this type of start by means of external forces, an especially

energy-consuming part of the aircraft acceleration is not obtained at the expense of the fuel carried on board, so that the range of the aircraft catapulted in this fashion rises markedly, while at the same time the flight-characteristics can be matched more easily to the steadily decreasing wing loading during flight.

As methods of flight were considered: acceleration to the point where flight speed equals exhaust speed, and then flight at constant speed; also acceleration to such a speed that the subsequent unpowered glide extends over the entire remaining flight path. For equal fuel cost, the last method gives greater ranges and simpler power plant, and is therefore assumed from now on.

The whole procedure for use takes place somewhat as follows: the rocket bomber at the surface of the earth is brought to a speed of about 500 m/sec. by a ground-fixed rocket drive in a period of 11 seconds over a 3 km. starting path; then climbs at full motor drive to a height of 50-150 km along a path which is inclined at 30° to the horizon at first, but later becomes flatter; thus it reaches final velocities up to more than twice the exhaust speed. The duration of the climb is 4-8 minutes; usually during this time all the fuel supply on board will be consumed. At the end of the climb the rocket motor is turned off, and the aircraft, because of its kinetic and potential energy, continues on its path in a sort of oscillating gliding flight with steadily decreasing amplitude of oscillation. This type of motion is similar to the path of a long-range projectile which from similar heights follows a descending glide-path. Because of its wings the aircraft descending its ballistic curve bounces on the lower layers of the atmosphere and is again kicked upwards, like a flat stone ricocheting on a water surface, though during the entrance into the dense air each time a fraction of the kinetic energy is consumed, so that the initially big jumps steadily become smaller and finally go over into a steady gliding flight. At the same time the-flight speed, along the glide path of several thousand kilometers, decreases from its high initial value to normal landing speed. If the descending path (which is within certain limits controllable by the pilot) lies in the direction of the target, the bombs are released at a predetermined moment, and the craft returns to its starting place (or some other landing field) in a wide arc, while the bombs go toward the target along the original direction of flight. Even if the target is very distant from the take off point, the bombs are only dropped near it, so that the scatter of bombs can be compensated for by a large number of releases on the target, which will in this way be covered by a Gaussian distribution of hits. This military use is completely independent of weather and time of day at the target, and of enemy counteraction, because of the possibility of using astronomical navigation in the stratosphere and because of the height and speed of flight.

From the characteristics given for the rocket bomber it follows that this is not the development of an improved military craft, which will gradually replace present types, but rather that a problem has been solved for which no solution existed up to now, namely, bombardment and bombing over distances of 1,000 to 20,000 km. With a single rocket bomber point attacks can be made, e.g. from Central Europe, on distant point targets like a warship on the high seas, a canal lock; even a single man in the other hemisphere can be fired upon.

With a group of 100 rocket bombers, surfaces of the size of a large city at arbitrary places on the earth's surface can be completely destroyed in a few days.

II. The Aircraft

1. Characteristics of the Rocket Motor

The main parts of the basic construction of the rocket motor considered here are shown in Fig. 1. The fuel goes from the fuel tank to the fuel pump, where it is compressed to 150 atm., then fed continuously through valve 5 to the injection head of the combustion chamber. The oxygen goes from the thin-walled uninsulated oxygen tank into the oxygen tank, is compressed to 150 atm. there, then forced through valve 6 and the pipe system of the condensers into the injection head and the combustion chamber, after being warmed to $0°$ C. There the fuels come together for the first time, mix and burn producing flue gases at a constant pressure of 100 atm. and at $4000°$ C. In the head of the burner, the flue gas expands to a very low pressure and forms the driving mass-jet with exhaust velocity of 3-4000 m/sec, whose reaction for a fuel consumption of 245-327 kg/sec produces a thrust of 100 tons. With a 90 ton fuel supply, the aircraft can be driven with the above thrust for 367-275 seconds.

Aside from this main process with energy conversion of about a million Kcal/sec the secondary process shown schematically in Fig. 2 gives an energy conversion of 20,000 Kcal/sec for driving the feed-pumps. Its parts, visible in Fig 1, can be followed from the water pump which puts about 28 kg/sec of water under 250 atm. pressure, drives this water, at the jet throat, into the cooling pipes of the jet walls, where it flows toward the mouth of the jet and is heated to about 300° C. After coming out of there, while still above the critical pressure, it is (again at the jet throat) driven into the cooling pipes of the combustion chamber wall, where it is again heated and vaporizes in the neighborhood of the critical pressure; finally it is removed at the injection head in the form of highly-compressed superheated steam, led to the steam turbine; there it expands to about 6 atm. and goes to the liquid-oxygen-cooled condensers where it is reconverted to water and gives up considerable energy to the oxygen; then it repeats its cycle going through the water pump. The steam turbine drives all three pumps from the same shaft. During the process valves 3, 4, 5, and 6 are open, and 1, 2 are closed, while 7 serves as a safety valve against too high rotation of the turbine.

The process described can be begun with the aid of the steam-starter, which produces the small amounts of steam required by chemical means; in this process the valves 3 and 4 are closed, 1, 2, 5, 6, and 7 are opened.

Aside from the details given in the literature, (16-30) the following things are important for understanding the proposed construction:

The relative value of different fire-wall materials is determined by the available heat flow $q = \lambda (t_f - t_k)/d$ through the walls for a given heat capacity of the walls. If the wall thickness d is proportional to the reciprocal of the breaking strength σ (tensile stress), or to its square root (torsion stress), then the possible heat flow (and also therefore the worth of the material) is proportional to the product $\lambda (t_f - t_k)/\sigma$, or $\lambda (t_f - t_k)/\sqrt{\sigma}$ resp. Here λ, t_f and σ are pure material constants, while the cool-surface temperature t_k (and so the whole evaluation) depends on the particular arrangement, coolant temperature, etc. In the combustion chamber cooled by live steam, the cool-surface temperatures are 500-600° C. From Fig. 3 one sees that the usual heat-resistant metals chrome-nickel steel, nickel, " ventil"-steel, etc., are favorable (as confirmed by construction experience) while platinum is even more suitable. The theoretically most favorable materials like tantalum, tungsten, and molybdenum are, because of their chemical activity and the difficulty in working them, actually not at all promising. In the hot-water-cooled fire-jet the cool-surface temperatures are at 400-500° C, because of the high heat flow; Fig. 4 shows (in accord with practical experience) that copper is unsurpassed as jet-wall material.

The cooling system for the walls in contact with the flame (21) is required because of the high heat flow from the combustion gases to the fire-walls; this is presented in Fig. 5 for a gas-oil-oxygen charge at 100 atm. combustion pressure, on the basis of calculations and practical experience. For example, in order to conduct 5 hp./$_{cm}2$ from the fire-surface to the cool surface through a 1 mm thick copper wall, a temperature gradient $(t_f - t_k)$ between the two surfaces of 100° C is necessary. In order for such thin walls to withstand the mechanical stresses due to flame-and coolant-pressures, they must be reinforced at very short intervals. At the same time the heat flow through the fire-walls must be assured by a precisely prescribed and carefully maintained high streaming velocity of the coolant behind the fire-wall. Both requirements can be met by the cooling-pipe system shown in Fig. 1, with forced circulation of the coolant in structures of one-dimensional extent. The necessary compromise between the rising forced motion and increased pressures required to drive the coolant when the number of channels is decreased has been so made that the cooling system of the jet consists of several hundred parallel pipes each only a few
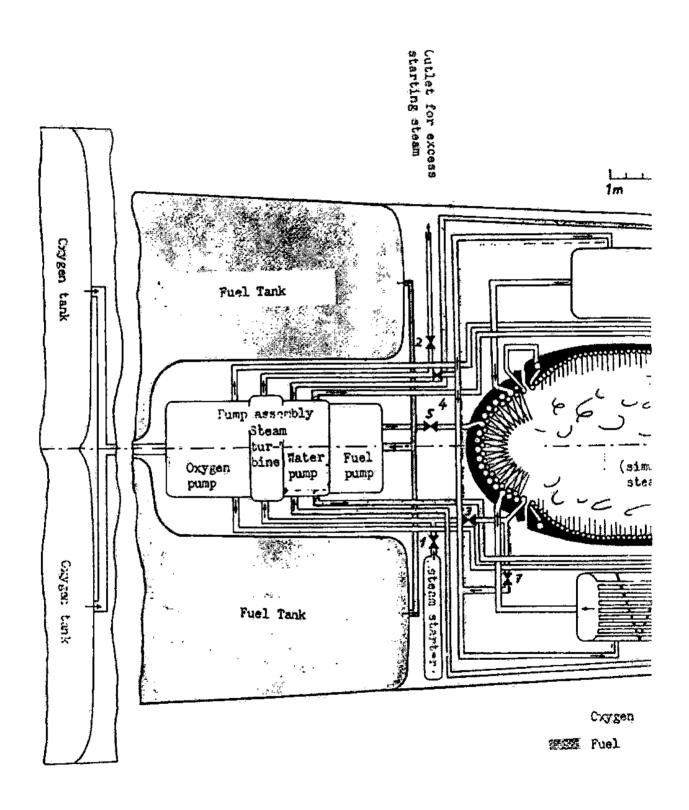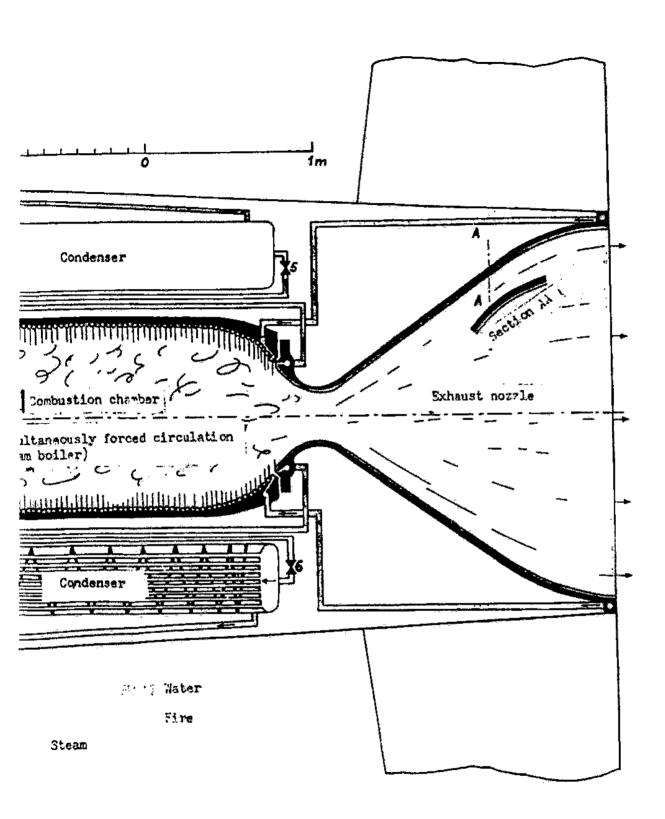
Fig. 1: Systematic representation of the main parts of the rocket mot of the rocket bomber.

0   1m

Condenser

X5

Combustion chamber

ıltaneously forced circulation
ım boiler)

A

A

Section AA

Exhaust nozzle

Condenser

X6

Water

Fire

Steam

or, drawn in the interior

MAIN PROCESS

PROCESS FOR PUMPWORK

Energy arriving
with the fuels
(~100%)

Energy in fuel
after pumps
(~100-2%)

Energy in fuel
after the con-
denser(~102%)

Total energy
flowing out
from the exhaust
(~100%)

Heat added to the fuels by
pumpwork (~2%)

Energy contained in the
steam after the turbine
and added to the fuel
by condenser (~18%)

Energy contained in the steam
before the turbine (~20%)

Heat conduction through walls
in contact with the flame
(~20%)

Fig. 2: Energy flow in the working process of the rocket motor.

9

sq. mm. in cross-section, which join together partially at the jet throat and again branch off
in the far parts of the jet mouth so that the small individual cross-section of the pipes is
retained; each pipe runs meridionally, and the whole surface of the jet is completely covered
with pipes, of which the side toward the flame consists of the smooth and torsion-stressed fire-
wall. The requirement of a plane surface does not apply to the furnace surface in contact with
the flame, so that there the statically more favorable circular cross-section can be used. This
circumstance and the smaller heat-flow through the furnace walls require greater wall-strengths
of the fire-wall and thus greater cross-section for the individual cooling pipes, so that the
then necessarily few pipes in parallel can assure high circulation of the coolant in the neigh-
borhood of the steam chamber which has varied and unstable flow conditions. These few cooling
pipes are wound on the furnace surface in the form of an evaporating coil.

We see, from the above discussion, the requirements on the coolant itself: large heat
capacity, heat conductivity and density; for this reason mercury has advantages over water.

The reason why the furnace-jet in Figs. 1, and 5 is shown with the unusually large open-
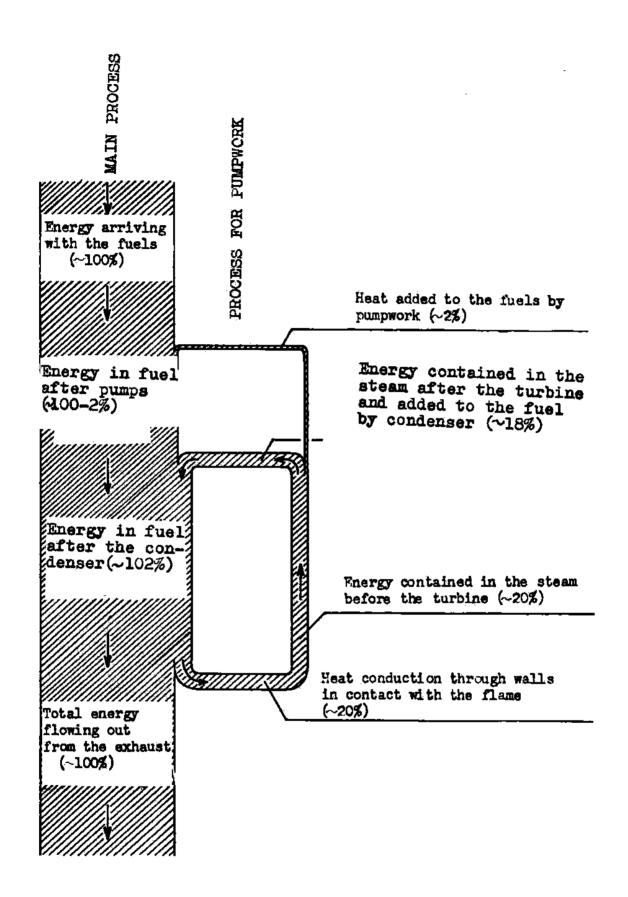ing angle of 60° is the following: (22) Aside from the fact that a special coolant, which best
suits the requirements, is circulated around the fire-walls, the actual coolant is really the
fuel itself, to which the intermediate coolant transfers its heat in the pumps and condensor.
The heat-absorptivity of the fuel before it is brought into the combustion chamber is limited,
and is only a few percent of the heat which is liberated when it is burned in the combustion
chamber. One must therefore take care, that the total heat transfer per sec. from the flue-gas
to the coolant through the walls of the furnace and jet, which is given as 20% in the example of
Fig. 2, remains less than or equal to the aforementioned absorptivity of the fuel consumed per
sec. This total heat transfer which must be regulated is proportional to the total inner surface
of the furnace and jet. It can be decreased by diminishing this total surface. Concerning the
contribution of furnace and jet to the total surface in contact with the flame, the following is
true: all experience shows that over a wide range of values, combustion in a furnace is more com-
plete, and efficiency and exhaust speed are correspondingly larger, the greater the furnace
volume Vo as compared to the smallest cross-section f of the furnace jet. Because the total wall-
surface is limited by the heat absorptivity of the fuel used as a coolant, the furnace surface
can be increased provided that the jet surface is decreased keeping the sum of the two below the
permissible limit. From Figs. 2 and 5, the total heatflow through the 154,000 cm of fire-wall
surface represents 2% of the energy developed, which corresponds to the permissible heat absorp-
tion of the fuel, so that the heatflow per unit area of the furnace and jet walls is about 0.8
np/cm^2. If in place of the short 60° throat with 60,000 cm^2 surface we used the customary Laval-
throat with a 10° opening angle, its surface (345000 cm^2) could not be completely cooled if the
same heatflow and absorptivity of the coolant were maintained; for the furnace there would be no
surface cooling available at all. At the same time the length of the Laval-throat could not be
decreased below 9720 mm. By using large throat-angles we are enabled to fulfil the requirements
of the fuel-cooled rocket motor, and moreover the quantity Vo/f which determines the completeness
of combustion can be increased, so long as the increased efficiency of the furnace J_b/E is not
overcome by the decrease of jet-efficiency $(Ac/2g)/J_b$ with increasing opening angle.

The pump system of the rocket motor consists of three pumps for fuel, oxygen and coolant,
and the driving turbine, for these pumps. The vaporized coolant of the rocket motor is used for
feeding the turbine, where the forced circulation used for the combustion chamber permits the
chamber to be used as a high-pressure-radiating-steam-boiler with forced circulation in the
manner of the Benson -, Lamont -, Velox -, Sulzer - steam boilers. (27) The use of the vapor-
ized coolant for driving the auxiliary turbine has the advantage over the use of a separate energy
source that the total fuel consumption per impulse by the rocket motor is not increased by the
auxiliary turbine drive; the advantages over feeding the auxiliary turbine from the flue-gas of
the rocket motor are that: use of the cooling capacity of the fuel for cooling the combustion
gases brings it to temperatures permissible for the turbine drive-rod; the difficulties associ-
ated with condensation of, for example, metallic-oxide fumes in the flue gas disappear; the heat
absorptivity of the fuel as a coolant is increased by the work done in pumping; the important
decrease in momentum of the jet in the emission of a part of the flue-gas and transfer of its heat
content to the remaining flue-gas is avoided; finally the construction of a high pressure steam
turbine is incomparably simpler than that of a high pressure flue-gas turbine. Since according to
Fig. 2, the efficiency of the 12,000 hp. drive of the steam turbine, which uses waste energy, i
unimportant, while we do demand very small weights of the installation, the simple Curtis-shaft
gives a suitable solution. The 3 pumps can in view of the high total fuel supply of over 1000
m^3/hr., be designed as one-stage turbines (despite the high intake pressures), so that the whole
pump assembly including the turbines consists of 4 running from the same shaft, at about 12,000
RPM. Thus the outer dimensions and weight of the whole installation can be kept below 600 x 1200
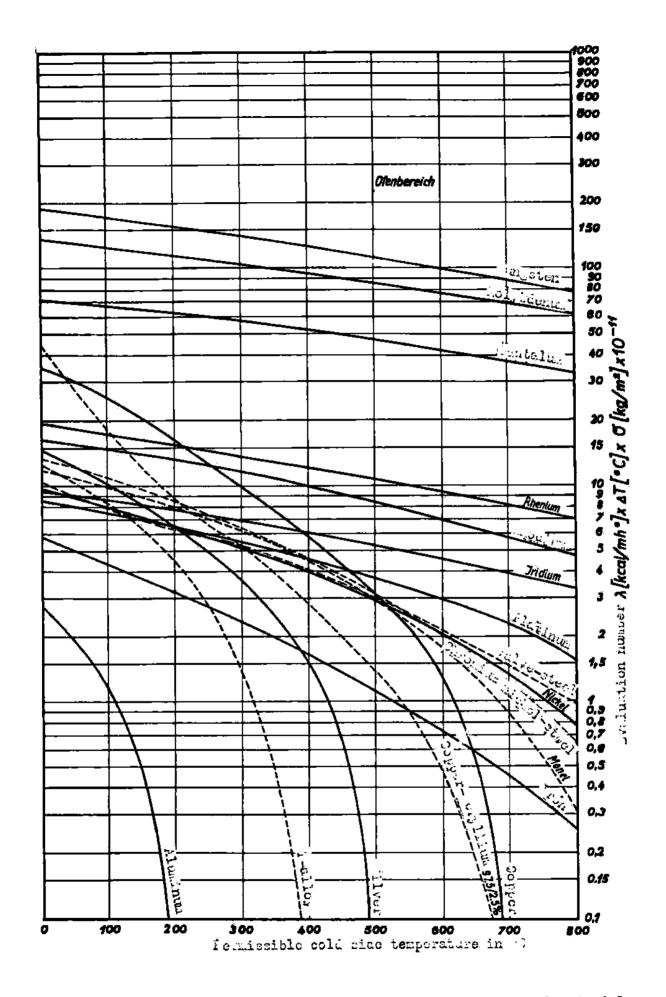mm and 500 kg.

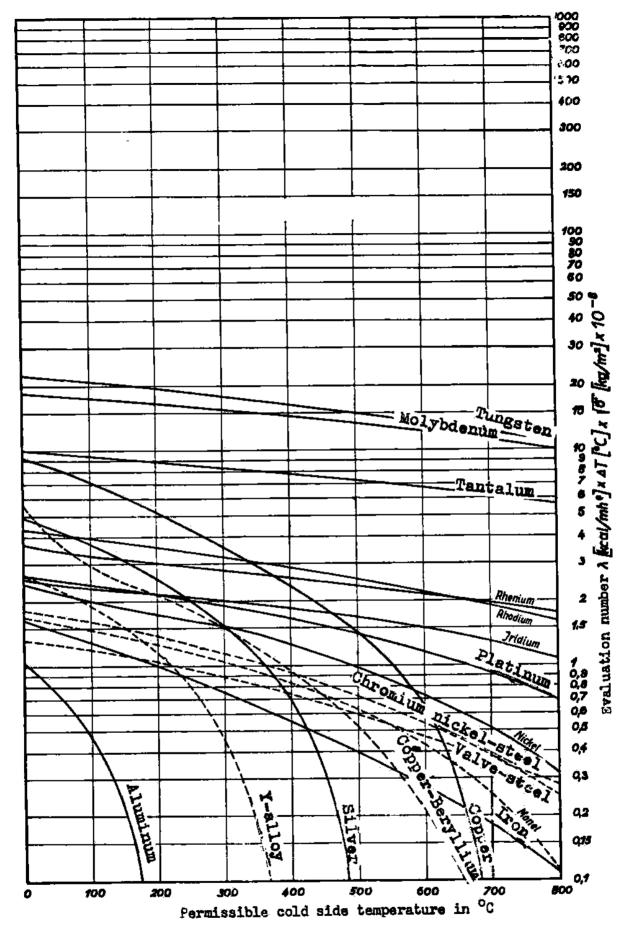**Fig. 3:** Relative evaluation number of combustion chamber wall materials subject to tension.

Fig. 4: Relative evaluation numbers of firewall construction materials under bending (exhaust wall materials).
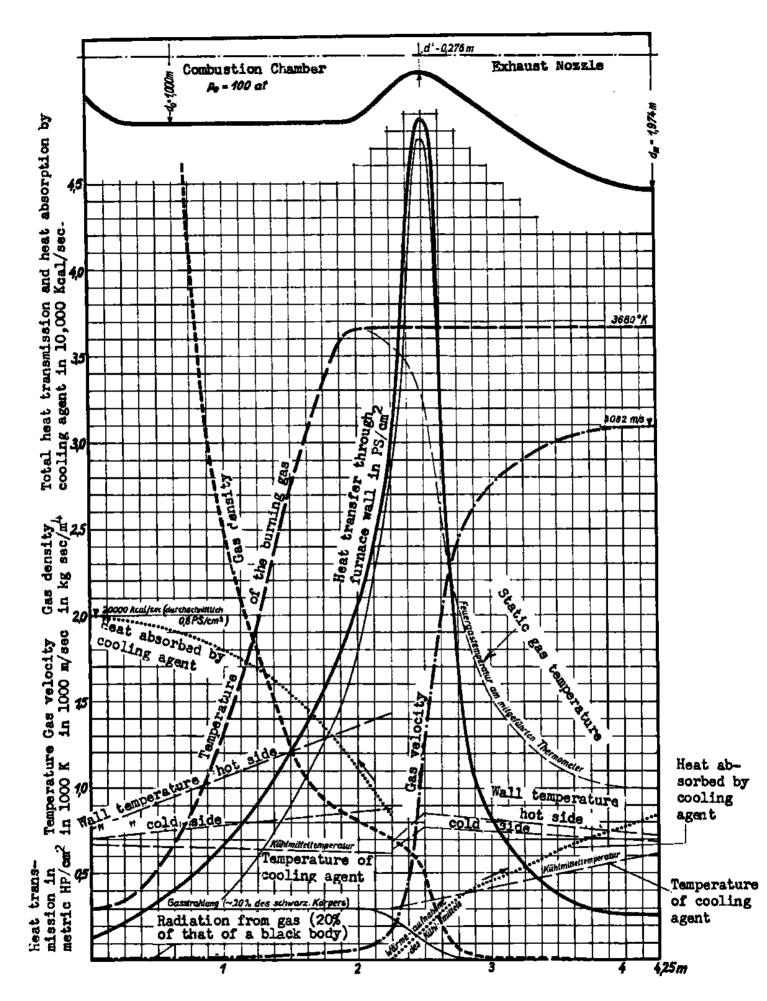
12

Fig. 5: Conditions in a 100 ton rocket motor operating with oxygen and oil.

Aside from the requirements of extremely light construction the turbine, fuel pump and water pump present no special constructional difficulties, whereas in the construction of the oxygen pump the choice of the construction material, the arrangement of the moving parts and the feeding of the boiling liquid to the pump must be specially considered. As a construction material (for the oxygen pump) which at -180° C will be sufficiently strong, elastic and resistant to impact, sufficiently resistant to corrosion and non-inflammable in liquid oxygen, the nickel-, Al-, and Mn- bronzes, as well as Monel-type alloys and pure nickel have proven satisfactory. In view of the inflammability of all lubricants in liquid oxygen, the problem of arrangement of moving parts was solved by using a floating support for the pump shaft away from the oxygen. In order to drive the boiling liquid O_2 from the tank steadily to the pump, an arrangement was used whereby the oxygen flows toward the pump over a long route in the direction of an acceleration field; a.g., in the test installation, from a higher level; or in the aircraft, from tanks lying far toward the front. Because of the gradual pressure increase in the feed lines, accompanied by only a slight temperature increase, supercooling of the O_2 occurs at the pump intake, so that no more gas is liberated.

Fig. 6 is a photo of the experimental model of a high-pressure liquid- O_2 pump, which as a rotary 6-stage pump with external bearings supplies 5 kg/sec of liquid O_2 at 150 atm. pressure, when running at 15,000 RPM; it has proven its suitability and reliability in hundreds of experiments.

The ignition of the rocket motor is not shown in Fig. 1, because ignition is limited only to starting; once the combustion chamber gets going it operates like a welding-burner. The basic ignition procedure chosen was the injection into the combustion chamber of materials which ignite on contact with O_2 or air. From the pyrophors to be considered, like the phosphorus hydrides, "silanen", halogen-acetylenes, rare earth amalgams, metal alkyls, etc., zinc-diethyl $Zn(C_2 H_5)_2$ was chosen at the suggestion of H. Troitzsch; F. Zohrer developed a suitable ignition fluid by dilution of this with heavy hydrocarbons (e.g., machine oil), and also an ignition apparatus in the form of a small pressure bomb using compressed nitrogen and a remote-controlled valve; by a simple movement of the valve and consequent injection of the ignition fluid into the combustion chamber, arbitrary ignition time and arbitrary repetition of the ignition is possible. This ignition procedure is notable for its sure performance and the very smooth starting of combustion.

The practical work on the development of the rocket motor described in this section was taken up by the senior author in 1933-34 at the Technische Hochschule in Vienna and gave in the first experiments, on small models with 30 kg. thrusts, controllable flame-pressures of 50 atm. and high exhaust speeds; the fuel was O_2 (at up to 150 atm. injection pressure), and gas-oil (at up to 500 atm. injection pressure), and a Laval-throat of small opening angle was used. (19) After a delay of several years, which were spent in constructing larger experimental installations, the tests were recommenced at the Trau Aeronautical Testing Station in 1939. The construction of the experimental installations was under the direction of H. Zborowski; the construction of the components was directed by H. Ziebland; K. Hedfeld directed the experimental work. Fig. 7 shows the testing-shed during an experiment with 1 ton thrust and 5 minutes duration. Among the important parts, one can see at the left on the embankment a cylindrical tank of capacity 2.5 m³ for the liquid O_2, and just to the right of it the tap for the underground tank of liquid O_2 (see also II, 2). The drive tank, from which the apparatus is directly fed, is an open uninsulated thin-walled metal tank which (out in the open) vaporizes oxygen at the rate of 15 kg/hr. per sq. meter of tank wall, and whose varying weight during the test is shown by an automatically-recording spring balance. From this tank the liquid O_2 flows at slow speed under its own weight to the high-pressure liquid oxygen pump 8 m. below (see fig.). Beyond the feed pump the liquid oxygen, now at 150 atm. pressure, runs through a heat exchanger, in which it is heated by the warm cooling-water coming from the furnace, then goes into the combustion chamber through a large number of injector nozzles. Following the corresponding path of the fuel, we see in the left foreground a 1m³ fuel tank, from which the fuel flows under its own weight to the high-pressure fuel pump. For this purpose a cog-wheel pump is used, which compresses the gas-oil to 150 atm. at 3000 RPM. In the experiment shown here, the fuel and oxygen pumps were driven together by a D.C. Motor standing between the pumps; later the coolant-steam turbine was used instead. Beyond the fuel pump the fuel also is forced into the combustion chamber through a large number of nozzles. The fuel - and O_2- streams are directed at 90° to each other and have initial entrance-velocities of about 100 m/sec so that rapid spraying and mixing is forced. In the furnace, the three fluids - oxygen, fuel and ignitor - meet and form the furnace gas. The furnace-gas pressure during the entire run is up to 100 atm. with $Vo/f = 800$ and about 30° opening angle of the provisional expansion-nozzle. The next photos 8 and 9 show a 1-ton trial from the jet side, 10 shows a small model using coolant vaporization; Fig. 11 shows a 1-ton trial in which a high-percent Al-gas-oil suspension was used as fuel. The flame glows brighter in this case, and the resulting aluminium oxide begins to condense to white corundum dust at a few meters from the jet opening, and then thickens into a heavy white cloud. Finally, Fig. 12 shows a short-exposure
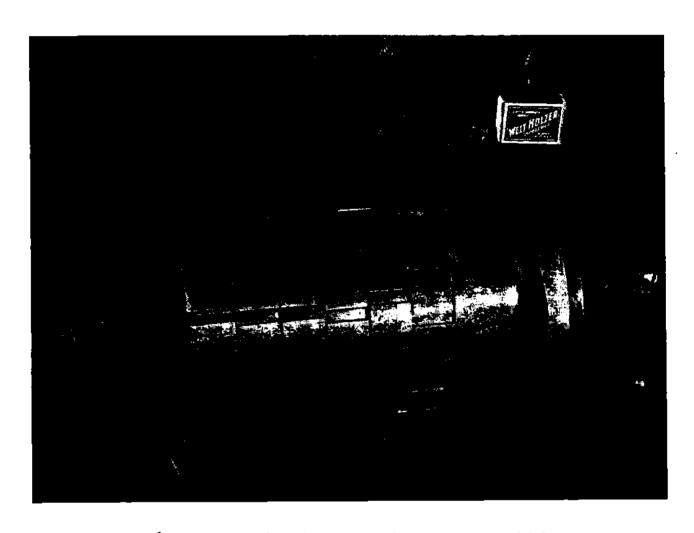
Figure 6: Experimental high pressure liquid O_2 pump which has a 6 stage rotary pump. At 15,000 R.P.M. it is pumping 5 kg/sec of liquid O_2 at 150 atmospheres.
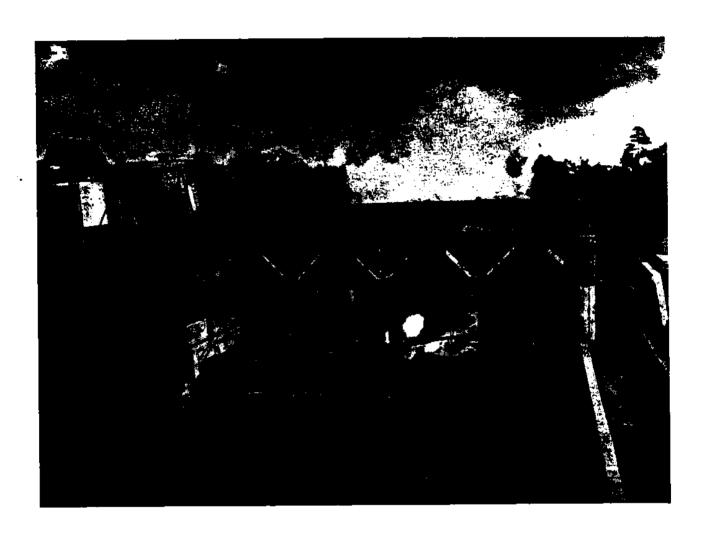
Fig. 7: Overall view of a 1-ton, high pressure combustion chamber experiment using cooling by evaporation. Propellent tanks are above roof to the left. The fuel pumps directly underneath. Combustion chamber is in operation in center. Note the cloud of condensed cooling agent. The observation stand is above on the right.

16

C-842
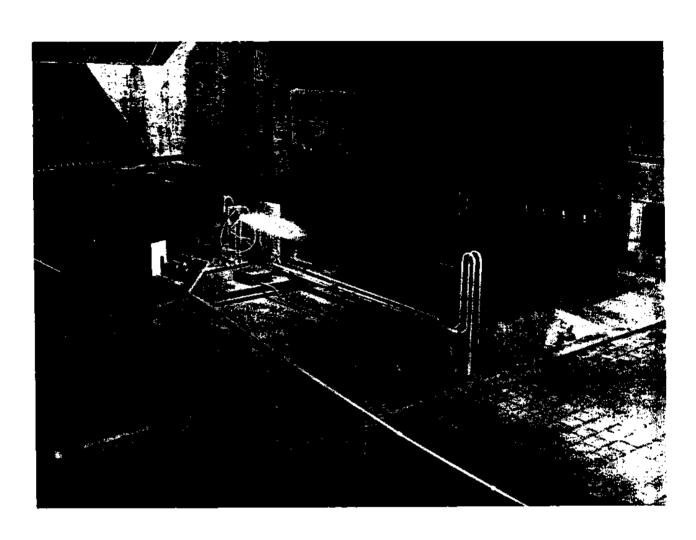
Figure 8; Overall view of a rocket motor test stand. This motor produced 1 ton of thrust for a duration of 5 minutes.
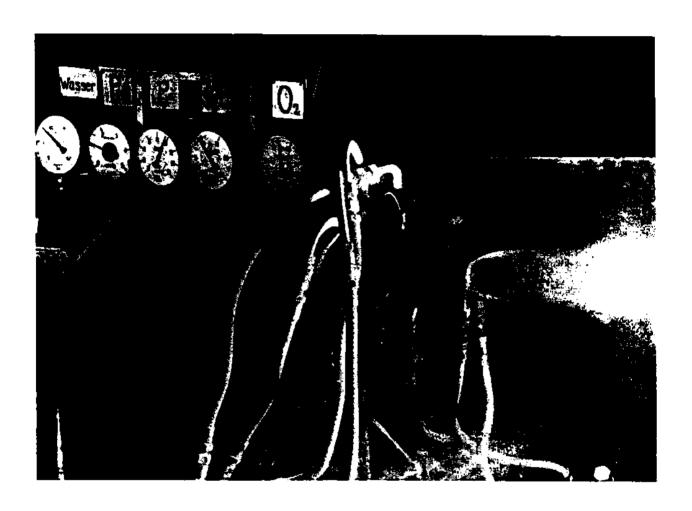
Figure 9; View of instruments and propellent lines. This
test was run on the 20th of March 1941. The
chamber pressure 100 atmospheres, the thrust 1.1
tons, the duration 3.5 minutes.
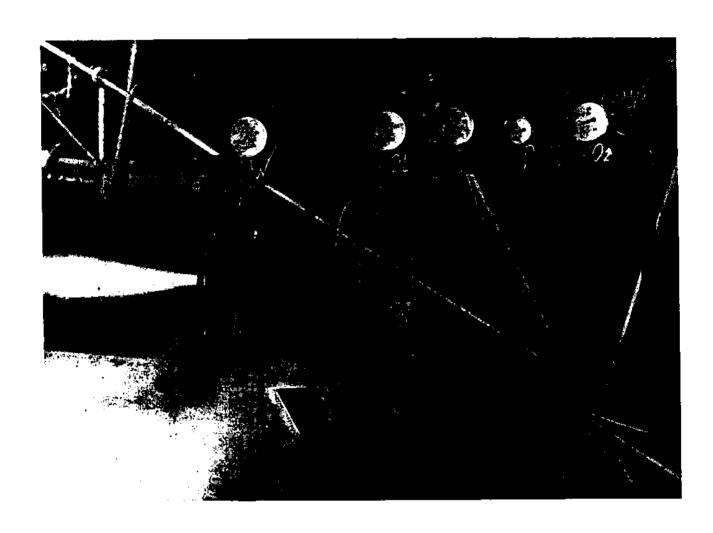
Figure 10; Small water cooled combustion chamber and test
instrument in duration test. Water, heated at
400° centigrade at 100 atmospheres pressure in
the cooling system.

19
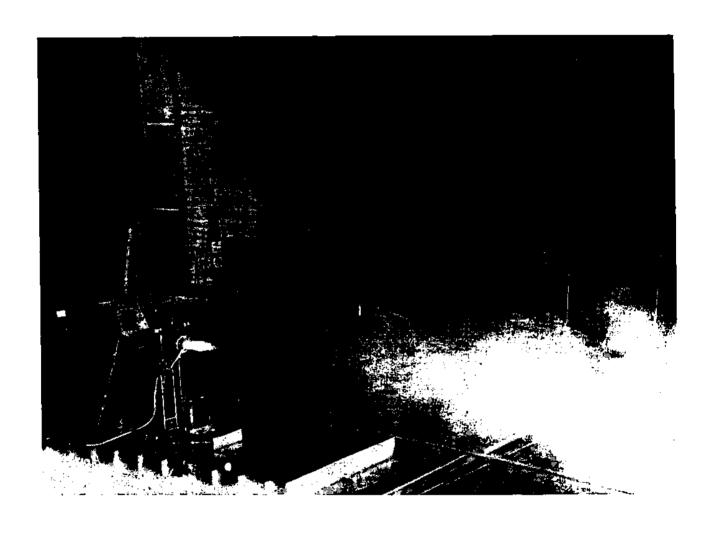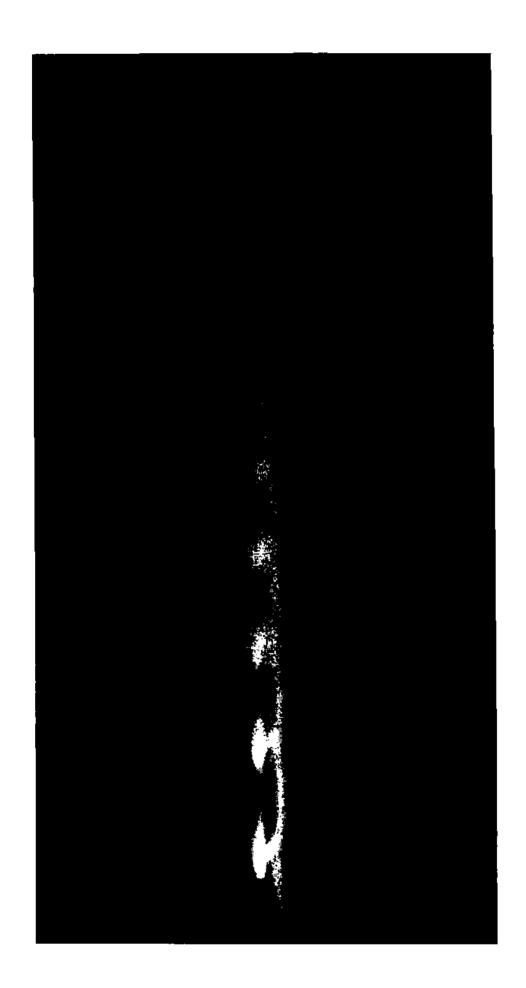
Figure 11; Rocket motor test stand experiment using Aluminum
in oil dispersion as fuel. Supersonic exhaust gases
from the nozzle of 1-ton experimental rocket motor.
Note compression **lines**.

Fig. 12: Supersonic exhaust gases from the nozzle of the rocket motor during an experimental run. Thrust was 1 ton. Note the compression lines.

21

Fig. 17a: Exper. construction of the evaporative cooling system of a 100 ton high pressure combustion chamber.

22

photo of the jet itself, in which one can see with the naked eye the supersonic compression lines which give the exhaust jet the appearance of a large, blue crystal.

The main part of the practical work consisted in the construction of combustion chambers for developing and withstanding of combustion gases with the high energy concentration mentioned. No time could as yet be devoted to the conversion of the heat into kinetic energy of a jet, that is to construction of a jet nozzle. Ordinary amounts of fuel consumption in the course of long and steadily run tests, gave effective exhaust speeds of up to 2400 m/sec at about 35 atm flame pressure, with gas-oil-oxygen fuel and for $k = O_2/f = 1.43$ (i.e., still insufficient performance of the extended throat section).

With the relatively low $\varkappa$-values of the combustion gas (about 1.25) carefully constructed fire-jets should, according to Fig. 17, give at least $P/p_{ef} = 1.6$ in the test set-up, and about $P/p_{ef} = 1.75$ in the aircraft, so that the combustion gas developed corresponds to effective exhaust speeds of 2700 m/sec. on the ground, and near 3000 m/sec. in the aircraft.

Finally, Fig. 12a shows a trial construction of the carburetor of a 100-ton rocket high pressure combustion chamber, which was not however used in the experiments.

2. Effective Exhaust-speed of the Rocket Motor

Statements concerning the form and nature of the physico-chemical processes in the jet of the rocket-furnace, which could give a determination of the effective exhaust speed, assume a knowledge of the processes and of the final state of the combustion gas in the furnace.

One may assume that most of the available time in the furnace space (about 75 millisec) is used up in processes of spraying, heating, vaporization, dissociation, turbulence and diffusion of the injected streams of fuel and oxygen; and only a small part of the time is used for the actual combustion and coming to equilibrium. The fully prepared and mixed fuel-, and oxygen-molecules (or - atoms) collide, and react with each other, but will immediately dissociate again if there is no means of transferring the liberated heat of reaction to internal degrees of freedom, to other bodies, or converting it to translational energy. The last possibility exists for a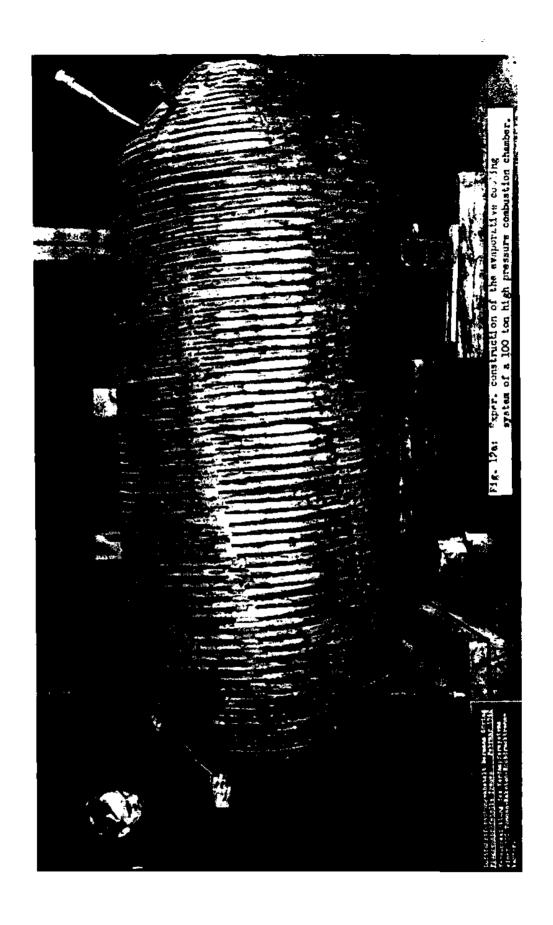tomic collisions (according to the principle of the conservation of the center mass) only if a third atom or molecule takes part in the collision, so that the particles present after the reaction can repel each other. (Triple collision, wall-catalysis, exchange reaction). A measure for the probability of occurrence of any reaction is the effective number of collisions, which states how many collisions of other particles with the molecule under consideration are required to produce the desired effect. According to an empirical formula of Geib (5) $Z_{\varkappa/5\varkappa}$ triple collisions occur in every Z ordinary collisions. After each formation of a new molecule, later collisions will supply energy first to its rotational and then to its vibrational degrees of freedom at the expense of its translational energy, till finally in some cases dissociation occurs. In the course of a sufficiently long time, which is dependent on the number of effective collisions which a molecule must undergo for each of these changes, and on the time interval between two such collisions, an equilibrium state (dependent on the pressure, temperature and proportions of fuel and O_2) develops in the furnace, which can be exactly described in terms of the kind, number and energy content of the molecules or atoms present. This state is assumed in the later calculations of the effective exhaust speed.

Since the greatest possible energy content of the translational degrees of freedom of the combustion gas determines the maximum possible value of the effective exhaust speed, one would prefer for the rocket motor a more favorable final state than that of stationary equilibrium, this seems to be attainable, since translation, rotation, vibration, dissociation and recombination take successively longer times to attain equilibrium, and the time during which the fuel remains in the furnace may lie anywhere between these times. According to Jost (8, page 141) it is conceivable that the newly formed molecules may, because of their process of formation, not have their vibrational degrees of freedom completely excited by the end of the combustion process, so that a greater fraction of the energy remains for the K.E. of the center of mass than corresponds to equilibrium; thus temperature and pressure at the end may be higher than that corresponding to equilibrium. (see K. Wohl and M. Magat, Z. Phys. Chem. Vol. 19, p. 117, 1932; also (10) p. 805, fig. 6, "The Approach to Thermal Equilibrium").

While, in the furnace of the rocket at say 100 atm. flame pressure and 3700° K, a molecule experiences an average of 10^{11} collisions per sec, the number of collisions drops after expansion in the jet, with a corresponding decrease in the rate of excitation of the degrees of freedom, the rates of further chemical reactions, such as reburning, and of physical reactions such as condensation or solidification of the combustion products (provided the temperature drops below their static sublimation temperature during the expansion).

The processes in the jet are then treated exactly as those in the furnace, neglecting all wall-effects; the expanding combustion gas is assumed to be an adiabatically closed system with a total energy E kcal/$_{kg}$ corresponding to the heat content of the mixture; i.e. $\Delta E = 0$

Accordingly as the time the streaming gas spends in the jet is long or short compared to the times of development of the various internal energetic and chemical equilibria, three assumptions are possible concerning the expansion:

1. The time spent. or the number of collisions which a molecule undergoes, on its path through the jet, is so small that no energy exchange or changes of vibrational and dissociation energy can occur. The characteristic conditions for this case are $dD = 0$ and $c_{v\,osc}\,dT = 0$; when put into the generally valid energy relations between total energy, E, heat supplied, Q, internal energy, U, heat of dissociation, D, heat of vaporization at $0°K$, R_{io}, heat content, J, work done in expansion, ApV, and kinetic energy Ac^2/g, to the equations:

$$dU = c_{v\,trans}\,dT + c_{v\,rot}\,dT = -A\,p\,dV;$$

$$\frac{p}{p_o} = \left(\frac{T}{T_o}\right)^{\frac{\varkappa_u}{\varkappa_u - 1}} \quad \text{where} \quad \varkappa_u = 1 + \frac{AR}{c_{v(trans+rot)}} \quad \text{is}$$

a "smaller" adiabat exponent which results from only translational and rotational specific heats; ($\varkappa$ ordinarily would be $(c_{v}rot + AR)/c_{v}rot$ (note by Transl).

$$\Delta J = \frac{\varkappa_u}{\varkappa_u - 1} AR(T_o - T) \quad \text{and}$$

$$c^2 = \frac{2g}{A}\Delta J = 2gR\frac{\varkappa_u}{\varkappa_u - 1}(T_o - T) = 2gRT_o\frac{\varkappa_u}{\varkappa_u - 1}\left[1 - \left(\frac{p}{p_o}\right)^{\frac{\varkappa_u - 1}{\varkappa_u}}\right]$$

gives the variation of the flow-velocity as a function of the pressure drop in the jet.

2. If the time spent by the combustion gas in the jet is such that vibrational states are instantaneously in equilibrium, whereas no chemical processes can reach equilibria corresponding to the changed conditions, then the flow is characterized by $dD = 0$, C_v osc. $dT = f(T)$. From this and the fundamental equations we get the relation:

$$\int_0^{T_o} C_{v\,osc}\,dT + (C_{v\,trans} + C_{v\,rot})\int_{T_o}^{T}dT = A\int_{V_o}^{V}p\,dV$$

For a gas mixture with $\underline{n}$ vibration frequencies and $\underline{m}$ different gases,

$$\overline{C_{v\,osc}} = AR\sum_{i=1}^{n}\left[\frac{(\theta_i/T)^2 e^{\theta_i/T}}{(e^{\theta_i/T} - 1)^2}\cdot\frac{p_i}{p_o}\right] \quad \text{and}$$

$$\overline{C_{v(trans+rot)}} = \sum_{i=1}^{m}\left[M_i C_{vi(trans+rot)}\frac{p_i}{p_o}\right]\Bigg/\sum_{i=1}^{m}\left[M_i\frac{p_i}{p_o}\right]$$

also $\overline{\varkappa_u} = 1 + \frac{AR}{\overline{C_{v(trans+rot)}}}$, where p_i is the constant

partial pressure of the gas as compared to p_o and θ_i the characteristic temperature. The integral for this type of flow is:

$$\frac{\overline{\varkappa_u}}{\overline{\varkappa_u} - 1}\left[\int_T^{T_o}\frac{dT}{T} + \sum_{i=1}^{n}\left[\frac{p_i}{p_o}\cdot\frac{1}{\theta_i}\int_T^{T_o}\frac{(\theta_i/T)^3 e^{\theta_i/T}}{(e^{\theta_i/T} - 1)^2}\,dT\right]\right] = \int_p^{p_o}\frac{dp}{p} \quad \text{and its solution is:}$$

$$\frac{\overline{\varkappa_u}}{\overline{\varkappa_u} - 1}\ln\frac{T_o}{T} + \sum_{i=1}^{n}\frac{p_i}{p_o}\left[\frac{\theta_i/T_o}{e^{\theta_i/T_o} - 1} - \frac{\theta_i/T}{e^{\theta_i/T} - 1} - \ln\frac{1 - e^{-\theta_i/T_o}}{1 - e^{-\theta_i/T}}\right] = \ln\frac{p_o}{p}$$

Furthermore

$$\Delta J = \frac{\overline{\varkappa_u}}{\overline{\varkappa_u} - 1}AR(T - T_o) + AR\sum_{i=1}^{n}\frac{p_i}{p_o}\theta_i\left(\frac{1}{e^{\theta_i/T_o} - 1} - \frac{1}{e^{\theta_i/T} - 1}\right)$$

and

$$c^2 = 2gR\left[\frac{\overline{\varkappa_u}}{\overline{\varkappa_u} - 1}(T_o - T) + \sum_{i=1}^{n}\frac{p_i}{p_o}\theta_i\left(\frac{1}{e^{\theta_i/T_o} - 1} - \frac{1}{e^{\theta_i/T} - 1}\right)\right]$$

3. The third possible type of flow in the jet occurs when the time spent in the jet by the combustion gas is so long that all energetic equilibria, including chemical equilibrium, can be attained for the instantaneous values of pressure and temperature. This type of flow is characterized by the conditions: $C_{v\,osc}\,dT = f(T)$, $dD = f'(p,T)$

24

From this and the fundamental equations, we obtain the differential equation:

$$d\left(\int_0^T C_p \, dT\right) + dD + A p \, dV = 0 \quad \text{or} \quad dJ + dD = ART \frac{dp}{p}$$

The function $dD = \psi'(p, T)$ which now contains M, cannot be represented in explicit form, so that no general analytic solution of the differential equation can be given. One must therefore, using the difference equation

$$\Delta J + \Delta D = ART \frac{\Delta p}{p} \quad \text{or} \quad J_1 - J_2 + D_1 - D_2 = 3.97 \frac{T_1 + T_2}{M_1 + M_2} \cdot \frac{p_1 - p_2}{p_1 + p_2} \quad \text{and}$$

as close a collection of values of J, D, and M as functions of p and T as possible, obtain the desired connections point for point. Procedures for calculating such tables for various fuels have been suggested by M. V. Stein.

The behavior of temperature T, heat content J, Dissociation energy D, and the liberated kinetic energy $Ac^2/2g$ along a pressure drop from $p_o = 100$ atm to $p_m \to 0$ for all three types of flow is shown for the combustion of octane in liquid oxygen in Fig. 13.
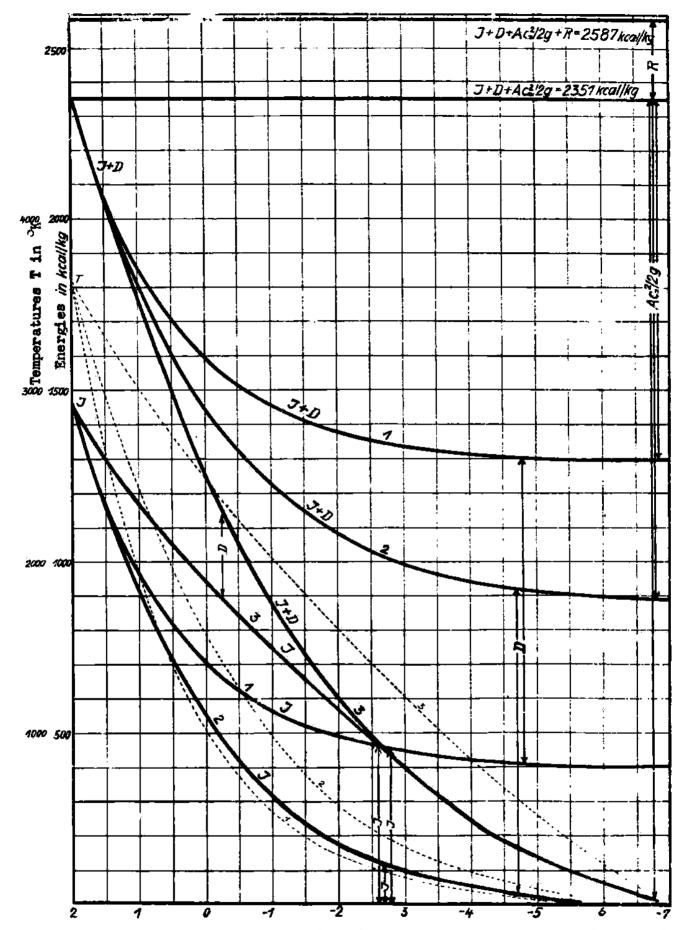
The decision as to which of the three possibilities (or an intermediate one) is most probable for the flow of the combustion gases from the rocket furnace is influenced by the following consideration: if the expansion takes place in an experimental short jet 1300 mm. long, then the mean time spent by the combustion gases can be computed to be about 2×10^{-3} sec, corresponding to an average no. of collisions of the molecule on its way through the jet of about 2×10^8. If one considers that 96% of these collisions already occur in the space between the furnace and the smallest cross-section, then one sees by comparison with the effective number of collisions $(10^2 - 10^3)$ for the various energy interchanges, that we may expect equilibrium of rotations, vibrations and possibly even dissociations for the processes occurring in the initial part of the jet, up to its smallest cross-section. Flow-type 1 becomes the more improbable the higher the furnace pressure and temperature for given velocity, the longer the jet, and the smaller the effective number of collisions of the combustion gas mixture. Therefore flow-type 2 is generally assumed in calculations on rockets; it gives closed integrable formulae. The actually rapidly varying $\varkappa$ can, for rough estimates, using the usual adiabatic flow formulae, be replaced in first approximation by a mean value $\varkappa^* = \frac{J/T_o}{J/T_o - AR}$ which for stochiometric burning of octane at 100 atm. gives $\varkappa^* = 1.248$

This mean value is strictly valid only for an expansion to $T_m = 0°K$ and $p_m = 0$ atm. If for example the mouth values are to be calculated for an expansion to $p_m = 1$ atm, then two equations are required for a determination of $/\varkappa^*/_{T_m}$ since both $/\varkappa^*/_{T_m}$ and T_m are unknown for a given mouth pressure $p_m \neq 0$. For the example of octane combustion given above, we obtain in this manner from the equations:

$$T_m/T_o = (p_m/p_o)^{/\varkappa^*/_{T_m} / [/\varkappa^*/_{T_m} - 1]} \quad \text{and}$$

$$/\varkappa^*/_{T_m} = \frac{J/T_o}{J/T_o - AR} = \frac{\frac{\varkappa_u}{\varkappa_u - 1} + \sum_a \left[\frac{b_i}{p_o} \cdot \frac{\theta_i}{T_o - T_m} \left(\frac{1}{e^{\theta_i/T_o} - 1} - \frac{1}{e^{\theta_i/T_m} - 1} \right) \right]}{\frac{\varkappa_u}{\varkappa_u - 1} + \sum_a \left[\frac{b_i}{p_o} \cdot \frac{\theta_i}{T_o - T_m} \left(\frac{1}{e^{\theta_i/T_o} - 1} - \frac{1}{e^{\theta_i/T_m} - 1} \right) \right] - 1}$$

for an expansion to $p_m = 1$ atm, the value $/\varkappa^*/_{T_m} = 1.222$ at $T_m = 1586°$ K. This method gives fairly accurate values of T_m and c_m whereas all intermediate values between T_o and T_m, as well as the corresponding c_m, are more inaccurate. Flow-type 3, in case its consideration can not be avoided, can be represented by the method of Mollier with the aid of entropy charts, which show $J + D + R$ as ordinate and enable c_m and temperature values to be read off. Figure 14 shows such a Mollier-diagram for a combustion gas of gas-oil-oxygen and gas-oil ozone respectively.

The following table shows in summary form for the case of stochiometric combustion of octane in O_2 at 100 atm. pressure, how the important final characteristics of the streaming: mouth velocity c_m, effective exhaust speed c, jet mouth temperature T_m, and the ratio of kinetic energy to total energy supplied (E), differ for the three types of flow and for different jet end-pressures.

Figure 13;   Temperature T, Heat content J, Dissociation loss Dpt, and
gain in kinetic energy plotted against the logarithm of the pressure
p according to the three possible streaming gradients in the nozzle.
(See text p.24 & FF).   The gasses entering the nozzle are assumed
to be a completely burned stoichiometric mixture of the octane and
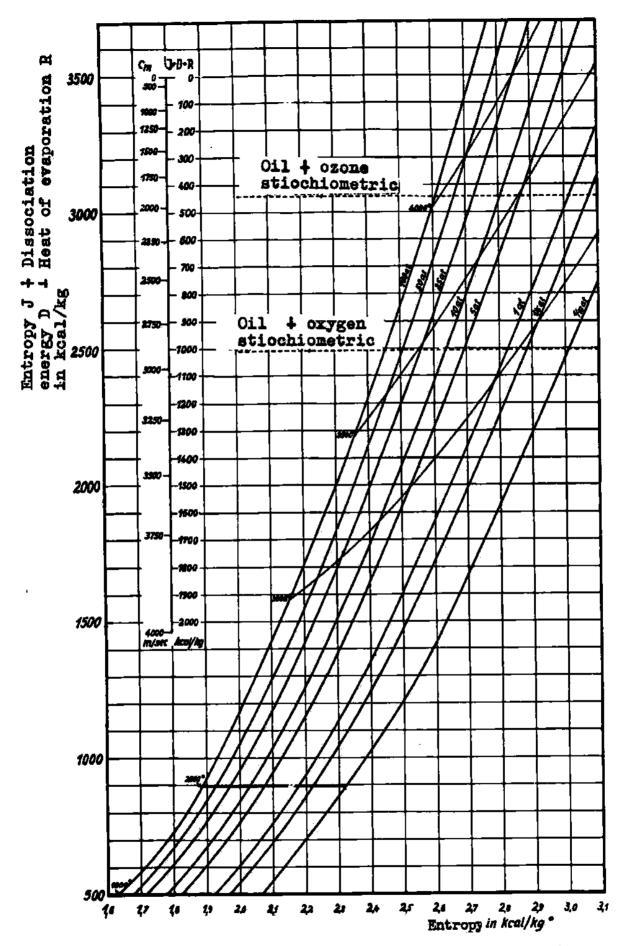O_2 at a pressure of 100 atmospheres.

Figure 14; Entropy diagram after M. von Stein for the Nozzle stream gradient and oil combustion.

Test stand conditions

	1	2	3
$p_m =$	1 at	1 at	1 at
$T_m =$	1030°K	1577°K	2500°K
$c_m =$	2518 m/sec	2759 m/sec	3020 m/sec
$c =$	2654 m/sec	2949 m/sec	3260 m/sec

Gained energy in the mouth of the nozzle in % of E.

	29.3	35.1	42

Flight conditions in d/dm =0.14:

$p_m =$	0.0729 at	0.1305 at	0.250 at
$T_m =$	500°K	1041°K	2225°K
$c_m =$	2760 m/sec	3066 m/sec	3330 m/sec
$c =$	2820 m/sec	3178 m/sec	3520 m/sec

Gained energy in the mouth of the nozzle in % of E.

	35.1	43.4	51

Optimum conditions in case of complete relaxation.

$p_m \rightarrow$	0 at	0 at	0 at
$T_m \rightarrow$	0°K	0°K	0°K
$\left.\begin{array}{l} c_m = \\ c_{max} = \\ c = \end{array}\right\}$	2970 m/sec	3496 m/sec	4438 m/sec

Gained energy in the mouth of the nozzle in % of E.
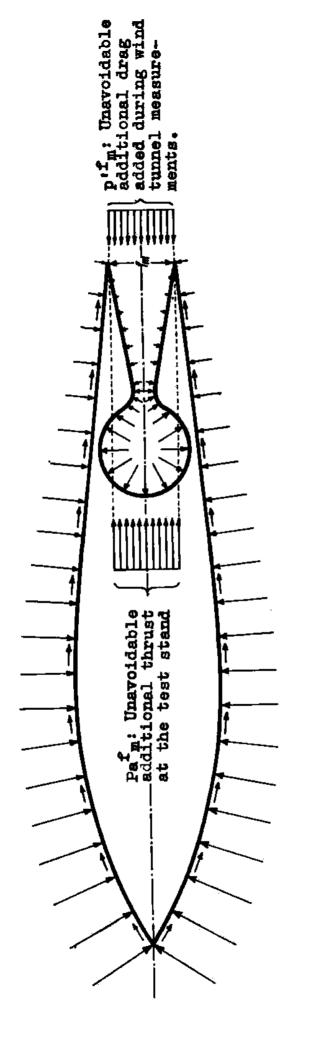
	40.7	56.5	90.9

Completely lossless conversion of the total input energy E into kinetic energy would give a theoretical exhaust speed

$$c_H = \sqrt{2g E/A} = 4655 \; m/sec$$

The concepts of mouth velocity c_m, maximal velocity c max, and effective exhaust speed c (19), require more detailed explanation. In general, for rough calculations, standard adiabatic-flow formulas, using a fictitious average $\varkappa$, whose magnitude and evaluation has been discussed already in presenting the three types of flow. Thus for expansion to a mouth pressure p_m, the mouth velocity is $c_m = \sqrt{\frac{2\varkappa}{\varkappa-1}\frac{p_0}{\rho_0}}$ for expansion to the theoretically possible limiting pressure $p_m = 0$, $c_{max} = \sqrt{\frac{2\varkappa}{\varkappa-1}\frac{p_0}{\rho_0}}$ and from these two relations:

$$\frac{c_m}{c_{max}} = \sqrt{1-\left(\frac{p_m}{p_0}\right)^{\frac{\varkappa-1}{\varkappa}}} = \sqrt{1 - T_m/T_0}$$

If we multiply the velocity c_m b the mass blown out per second dm/dt we obtain the mouth-momentum J_m of the jet.

In experiments with rockets, if the mouth pressure p_m in the jet is equal to the pressure of the surrounding still air p_a this mouth momentum is directly recorded by a dynamometer as the force P^s; it depends on the ext nal air pressure, i.e. on the barometer reading, altitude of the testing-place, etc. and must not be confused with the thrust P, as can be seen from a considera-tion of Fig. 15. There the conr tions between resistance and thrust for a flying apparatus and their values measured on he gr und are schematized.

By resistance to   e driven apparatus in flight we mean the vector sum of all the aero-dynamic forces on the ae ated surfaces. Let W be this sum of all the pressures and frictional forces. In a wind tunnel or a tow test on a non-driven device one always measures a smaller resistance $W' = W - p' f_m$, where p' is the absolute air pressure beyond the mouth surface f_m of the jet. It follows therefore that $W = W' + p' f_m$. For the moving body, the air pressure p' behind the

28

p'f_m: Unavoidable additional drag added during wind tunnel measurements.

Pf_m: Unavoidable additional thrust at the test stand

Figure 15: Relationship between thrust and drag in flight compared to sea level test values.

C-84296

rear surface is always smaller than the pressure p_a of the air at rest; for $v_0 > \sqrt{2/(\varkappa-1)} = 2.2, p' = 0$
The value p' must always be included in resistance measurements on undriven devices, in order to obtain the true resistance W of the body.

By thrust on an apparatus in flight we mean the vector sum of all the flame pressures on the surface of the rocket in contact-with flame (inner walls). In a test one always measures a smaller thrust $P' = P - p_a f_m$ where p_a is again the pressure of still air. The thrust measured in a test depends on the pressure of the surrounding air, and for the effective thrust we obtain $P = P' + p_a f_m$.

The effect of these two unavoidable additional effects in a wind-tunnel or a test can be seen most clearly by calculating the resultant force (thrust-resistance) which accelerates a mass $m = G/g$:

$$ m\, dv/dt = P - W = P' - W' + f_m (p_a - p') $$

For measurements on the ground, an unavoidable additional force proportional to f_m is thus included, which is different in measurements of resistance and thrust, and for which special correction must be made. The correction is small at moderate velocities (e.g. in the use of rockets for takeoff) and becomes largest for very high supersonic speeds (e.g. rocket projectile, long distance military rocket aircraft).

In order to calculate the effective thrust P of a rocket motor, one must add to the mouth impulse $J = c_m \frac{dm}{dt}$ the total pressure of the combustion gas on the jet mouth ($p_m f_m$); or one must add to the free dynamometer thrust in the test

$$ P' = J_m + f_m (p_m - p_a) = c_m \frac{dm}{dt} + f_m (p_m - p_a) $$

the total thrust of the still air on a surface the size of the jet mouth:

$$ P = P' + p_a f_m = J_m + p_m f_m = c_m \, dm/dt + p_m f_m $$

In the initially mentioned, most frequent case $p_a = p_m$, mouth impulse J_m and dynamometer reading P' are identical.

Thus the effective velocity c, which is independent of external air pressure, and which when multiplied by $\frac{dm}{dt}$ gives the effective thrust is:

$$ c = c_m + p_m f_m \, dt/dm = c_m + \frac{p_m}{\frac{dm}{dt} c_m} $$

and further

$$ c/c_{max} = \sqrt{1 - \left(\frac{p_m}{p_a}\right)^{\frac{\varkappa-1}{\varkappa}}} \left[1 + \frac{\varkappa-1}{2\varkappa} \frac{(p_m/p_a)^{\frac{\varkappa-1}{\varkappa}}}{1 - (p_m/p_a)^{\frac{\varkappa-1}{\varkappa}}} \right] $$

The determination of the effective exhaust speed c has the following peculiar, technically interesting consequence: in the usual engine construction the thermal efficiency is $\eta_{therm} = c_m^2/c_{max}^2 = 1 - T_m/T_0$ In the rocket motor the quantity which corresponds to this is the jet efficiency:

$$ \eta_D = c^2/c_{max}^2 = (1 - T_m/T_0)\left(1 + \frac{\varkappa-1}{2\varkappa} \frac{T_m/T_0}{1 - T_m/T_0}\right)^2 $$

(see also (19) p. 6). This expression implies that the higher temperatures and the quantities of heat at those temperatures are more "effective" than lower temperatures and quantities of heat at lower temperatures. This represents no contradiction to the energy theorem, since the effective exhaust speed is not identical with the actual velocity of flow of the combustion gas, but is <u>larger</u> than it. This relation has nevertheless a technical value, because the part of the initial heat content at lower (temp.) ranges can be made available only by special technical procedures (for gases, which soon tend to develop degeneracies, like condensation, it can't be done at all) and non-availability therefore leads to relatively smaller losses than one would expect according to the second law, for the non-available heat content.

Aside from the relations already given, we can, from the well known equation for the rate of gas flow through the jet throat

$$ \Delta G = \gamma' a' f' = f \left(\frac{2}{\varkappa+1}\right)^{\frac{1}{\varkappa-1}} \sqrt{2g \frac{\varkappa}{\varkappa+1} p_0/v_0} $$

and the equation for the effective exhaust speed, obtain a frequently useful relation between P, f' and p_0 in the form $P = k p_0 f'$ where

$$ k = 2 \left(\frac{2}{\varkappa+1}\right)^{\frac{1}{\varkappa-1}} \sqrt{\frac{\varkappa^2}{\varkappa^2-1}\left[1 - \left(\frac{p_m}{p_a}\right)^{\frac{\varkappa-1}{\varkappa}}\right]} \left[1 + \frac{\varkappa-1}{2\varkappa} \frac{(p_m/p_a)^{\frac{\varkappa-1}{\varkappa}}}{1 - (p_m/p_a)^{\frac{\varkappa-1}{\varkappa}}}\right] $$

By means of this factor k, by which the effective thrust is greater than the product of furnace pressure and jet-throat surface, one can reduce the otherwise tedious determination of effective thrust of a rocket motor, for sufficiently lengthened jet, to a measurement of the furnace pressure and the outside pressure, which can be easily done with ordinary manometers. This type of thrust measurement is very convenient in trial setups as well as in measurements on aircraft in

30

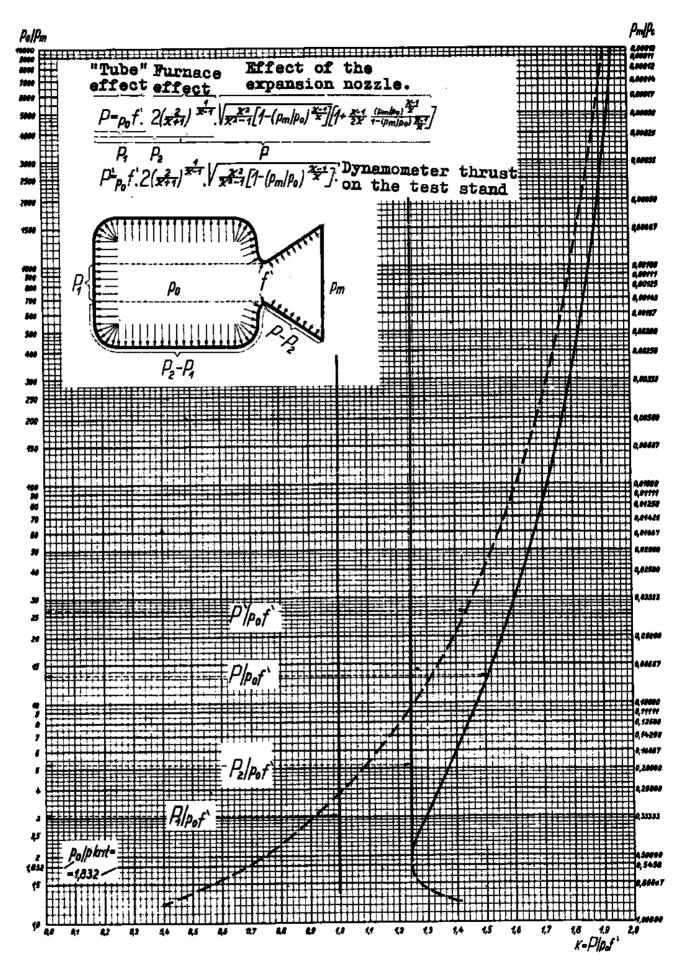Figure 16; Firegas flow with x=1.25

Figure 17; Analysis of effective thrust of rocket motor with x = 1.

flight. Conversely, in a test, if furnace pressure and effective thrust (or dynamometer thrust) are measured, the actually effective $\varkappa$ can be determined.

All these relations: the factor k, the ratios c/c_{max}, c_m/c_{max}, c/c_m, T_m/T_0 and d'/d_m are shown in Fig. 16 as functions of the ratio of furnace pressure to mouth pressure, for a frequently used value of $\varkappa = 1.25$.

As is shown in Fig. 17 for the special case $\varkappa = 1.25$, the individual factors in the expression for k can be interpreted very intuitively; the total thrust P of the rocket motor is made up of the partial thrusts: $P_2 = p_* f'$, arising from the pressure p_* of the combustion gas on that spot, f', of the rear wall of the furnace which one sees when looking down the axis of the jet, throat. A cylindrical tube, closed at one end, would show this same effect; $P = p_* f' \cdot 2\left(\frac{2}{\varkappa+1}\right)^{\frac{\varkappa}{\varkappa-1}}$, the increase relative to P_1, arises from the non-uniformity of the pressure distribution on the remaining furnace-wall surfaces due to the pressure gradient in the direction of the jet opening:

$$P_3 = P = p_* f' \times 2\left(\frac{2}{\varkappa+1}\right)^{\frac{1}{\varkappa-1}} \cdot \sqrt{\frac{\varkappa^2}{\varkappa^2-1}\left[1-\left(\frac{p_m}{p_*}\right)^{\frac{\varkappa-1}{\varkappa}}\right]}\left[1+\frac{\varkappa-1}{2\varkappa}\frac{(p_m/p_*)^{\frac{\varkappa-1}{\varkappa}}}{1-(p_m/p_*)^{\frac{\varkappa-1}{\varkappa}}}\right]$$

This increase relative to P_2 is caused by the pressure of the combustion gases against the extended jet.

The free thrust P' of the rocket motor is

$$P' = \Delta\frac{G}{g}c_m = p_* f' 2\left(\frac{2}{\varkappa+1}\right)^{\frac{1}{\varkappa-1}}\sqrt{\frac{\varkappa^2}{\varkappa^2-1}\left[1-\left(\frac{p_m}{p_*}\right)^{\frac{\varkappa-1}{\varkappa}}\right]}$$

and is shown for comparison in Fig. 17 by the dotted curve.

Before these physical considerations on chemico-energetic problems are treated in relation to the effective exhaust speed, we want to discuss briefly their significance in terms of the long-range rocket-bomber project. The familiar relation, that jet and rocket motors produce their energy conversion most effectively when the velocity of flight is (as closely as possible) equal and opposite to the velocity of the jet, might lead us to the false conclusion that the exhaust speed should be adjusted to the instantaneous velocity of flight. Since in the aircraft what matters is not ideal energy conversion per sec, but rather the smallest consumption of fuel in terms of weight, fuels with higher energy content, which give larger c-values, are to be preferred, even when this greater energy content per unit weight is not used so effectively. For a given consumption (of fuel) by weight, the energy given to the aircraft becomes greater, the greater the value of c, because the useful part $\eta_0 = 2\frac{v}{c}\left(1+\frac{v}{c}\right)$ of the driving energy $c^2/2$ from a unit mass of fuel ($i.e.$ $\frac{vc}{g}c^2$), increases rapidly with exhaust speed. Despite this, the great importance of the exhaust speed may be limited if the fuel having higher exhaust speed has other disadvantages. For example, a 50% aluminium-gasoil suspension and oxygen, having a tank volume per kg. fuel requirement of 0.84 dm, is preferable despite the somewhat lower exhaust speed, to liquid H_2 and O_2, which requires $2.4dm^3$ tank space per kg. of fuel, and for which moreover special heavy devices are needed in the tank space because of the low temperature of the liquid H_2. The following general statement can be made concerning the effect of density on the choice of fuel: if the flight path s is approximately proportional to the cube of the maximum flight velocity v, and v is related to the exhaust speed c and weight ratio G/G_0 by the equation of page 207, $v = 0.443c + c \ln G_0/2G$, then $s = const. \times c^3 \times (\ln\frac{G_0}{G} - 0.25)^3$. One can therefore obtain equal ranges for different values of c, if G/G_0 varies properly. By differentiating (keeping s, v, and G_0 constant) we obtain $\frac{\Delta c}{c} = \frac{s}{v}\Delta\frac{G}{G}$ A dependence of the expression $\Delta\frac{G}{G}$ on the small change ΔE_v in the energy density E_v can be estimated as, for example, $\Delta\frac{G}{G} = -0.5\frac{\Delta E_v}{E_v}$ Thus $\Delta\frac{c}{c} = -0.5\frac{s}{v}\cdot\Delta\frac{E_v}{E_v}$, so that in the region of interest, $\frac{s}{v}\approx 0.5$, $\frac{\Delta c}{c}\approx-\frac{1}{4}\frac{\Delta E_v}{E_v}$. Variations in exhaust velocity are four times as effective as improvements in density. Furthermore these considerations permit a comparative evaluation of different fuels, by starting from a standard fuel, say a hydrocarbon with liquid oxygen, having values c and E_v. From these and the corresponding c_i and E_{v1} of the comparison fuel, an evaluation number K can be given in the form;

$$K = \frac{s_i}{s} = \left[\frac{c_i}{c}\cdot\frac{\ln\frac{2}{1+E_v/E_{v_i}}\cdot\frac{c_i}{c}-0.25}{\ln\frac{G_0}{G}-0.25}\right]^3, \text{ or, for } \frac{G_0}{G} = 10 \quad K = \frac{[2.746-\ln(1+E_v/E_{v_i})]^3}{8.650}\cdot\frac{c_i^3}{c^3}$$

A typical hydrocarbon reaction is the burning of octan in oxygen:

$$C_8H_{18} + 12\tfrac{1}{2}O_2 = 8CO_2 + 9H_2O + 2587 \, kcal/kg; \quad c_{th} = 4655 \, m/sec \quad [11]$$

The value for the upper limit of the heat of mixing is referred to $0°K$. From Fig. 18, it is clear that we must subtract from this value the 9.1% loss due to heat required for physical separation (melting, vaporization) and that the pressure dependent losses due to chemical separation (dissociation) amount to 34.4% at 100 atm. furnace pressure, so that under these driving conditions the furnace efficiency is $\eta_0 = J_0/E = 0.565$ This graph of octane combustion at
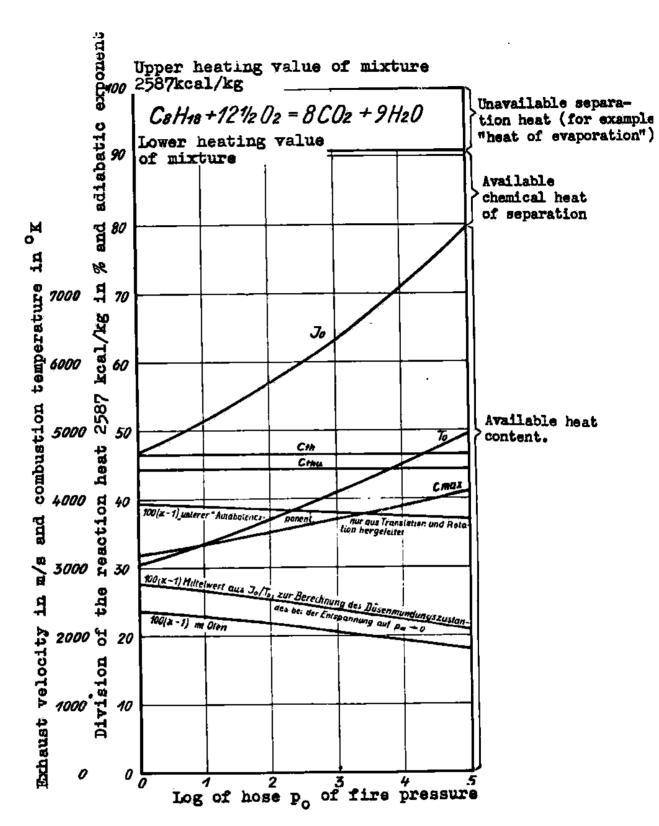
Figure 18; Heat of evaporation, dissociation, enthalpy, firegas temperature, theoretical and maximum exhaust velocity and adiabatic gas exponent of the combustion products in the case of oxygen and octane with static equilibrium.

34

varying furnace pressures, as well as the later graphs and tables for other fuels, were calculated by M. V. Stein, taking account of all the dissociation products, and assuming that physical and chemical equilibrium are reached in the furnace, and that expansion can be followed, as a flow of the second kind, to an external pressure zero. In addition the lower limit of the heat developed by the mixture $(E-R_{io})$, the heat content J_o, furnace temperature T_o, theoretical and maximum exhaust speeds are plotted, as a function of the log of the furnace pressure, for the proper average $\varkappa$ corresponding to this expansion; also to give some idea of the range of variation of $\varkappa$ for other types of expansion and other jet-mouth pressures, the adiabat exponent corresponding to the instantaneous furnace-state is shown as an upper value, and the value of $\varkappa$ for the calculations of flow-type 1 is shown as an upper limit. In this and the later graphs, which enable only a relative comparison of different fuels, the effective exhaust speed c, which is the determining factor for flight, and whose value for octane combustion has been previously given, is not especially noted. It can be determined from the maximal velocity using the value of jet efficiency:

$$\eta_b = (c/c_{max})^2$$

The expression for the total loss of the rocket motor is

$$\eta_i = \eta_o \cdot \eta_b = \left(\frac{c}{c_{th}}\right)^2 \left(\frac{c}{c_{max}}\right)^2 = \left(\frac{c}{c_{th}}\right)^2$$

numerically, for octane combustion at 100 atm. furnace pressure, $\eta_i = 0.565 \times 0.825 = 0.465$
The flight is fixed in this and all the later calculations by $d'/d_m = 0.14$, on the basis of the following consideration: in flight, the pressure behind the stern of the rocket bomber drops below 1 atm, so that the pressure gradient p_o/p_m at say 100 atm furnace pressure must go far above 100. The combustion gas will actually spread over the whole 2.50 m^2 surface of the stern of the aircraft; i.e., the ratio of jet mouth surface f_m to the jet throat surface f' will be about 50; throughout the working period of the rocket motor, corresponding to $d'/d_m = \sqrt{\frac{1}{50}} = 0.14$.

In addition to the important and carefully studied hydrocarbon-oxygen mixture, there is a second group of rocket fuels, having the common property that they are elements in the first columns of the periodic table, and which when burnt in O_2 give much higher energy concentrations per unit mass, and also generally per unit volume, than the hydrocarbons.

The following reactions were considered:

Untersucht wurden folgende Reaktionen:

Be	$+ 0.5\ O_2$	$=$	BeO	$+ 5930$ kcal/kg	bei $0^\circ K$;
2 B	$+ 1.5\ O_2$	$=$	B_2O_3	$+ 4930$ kcal/kg	" " ;
2 Li	$+ 0.5\ O_2$	$=$	Li_2O	$+ 4750$ kcal/kg	" " ;
2 Al	$+ 1.5\ O_2$	$=$	Al_2O_3	$+ 3920$ kcal/kg	" " ;(6, 13, 14)
H_2	$+ 0.5\ O_2$	$=$	H_2O	$+ 3900$ kcal/kg	" " ;
Mg	$+ 0.5\ O_2$	$=$	MgO	$+ 3330$ kcal/kg	" " ;

Combustion of Al and H_2 are shown in Fig. 19 and 20 in the same form as for octane combustion. The following table gives the most important characteristics for these light-metal-fuels with stochiometric liquid O_2 at 1, 10, and 100 atm. furnace pressure:

Upper value of heat of mixture E [kcal/kg]		BeO	B_2O_3	Li_2O	Al_2O_3	H_2O	MgO
		5930	4930	4750	3920	3900	3330
Heat of Vaporisation R_{io} [kcal/kg]		5040	2300	2780	1290	750	3750
Weight of Solid-Liquid Phase in Combustion Gas	at 1atm	13.8	-	-	-	-	43.0
	at 10 atm	18.0	-	-	-	-	48.0
	at 100 atm	23.2	-	-	-	-	54.5
Heat Content J_o in % of E	at 1 atm	20.6	40.5 .	21.9	21.5	45.8	28.7
	at 10 atm	23.8	46.7	24.1	24.4	51.7	35.0
	at 100 atm	28.4	51.4	27.0	28.1	59.7	44.1
Boiling Point at 1atm [$^\circ K$]		3400	1990	1100	3250	373	3120

	BeO	B_2O_3	Li_2O	Al_2O_3	H_2O	MgO
Furnace Temperature T_0 [°K] at 1atm	3400	6210	2350	3700	2950	3350
at 10atm	3920	7010	2730	4070	3200	3970
at 100atm	4550	7680	3200	4700	3560	4850
$\varkappa$ or $\bar{\varkappa}$ at 1atm	1.24	1.125	1.320	1.280	1.300	1.11
at 10atm	1.22	1.110	1.315	1.260	1.250	1.10
at 100atm	1.20	1.100	1.310	1.240	1.220	1.08
c_{th} [m/sec]	7050	6420	6310	5730	5720	5280
c_{max} [m/sec] at 1atm	3200	4090	2950	2660	3870	2830
at 10atm	3440	4390	3100	2830	4110	3130
at 100atm	3760	4610	3280	3030	4420	3510

In this calculation all heats of fusion were neglected relative to heats of vaporization; all possible dissociations of the end products of combustion were taken into account.

B, Li, Al and H_2 do not differ essentially from hydrocarbons in their behavior during combustion, but differ only in the numerical results; for example, Li and Al, despite their higher heat production, reach lower maximal exhaust speeds than for hydrocarbons, because of the vaporization and dissociation losses. Be and Mg are basically different. In the case of Be, the large heat of vaporization of BeO permits only a part of the burning mass to vaporize, while a large part remains in the liquid state (fog) or solid state (dust). These parts can then make use of the upper limit value of the heating value of the mixture, so that despite the large heat of vaporization, high temperatures, and high heat content of the total mass occur, with consequent large values of c_{max}. These liquid and solid masses in the combustion gas have a great effect on the expansion of the total mass, which expresses itself in the form of a very small adiabat-exponent. This $\bar{\varkappa}$ of the total mass is calculated from the weight fraction k_g of the gas phase, the weight fraction k_f and specific heat c_f of the liquid-solid phase by the equation:

$$\bar{\varkappa} = \frac{k_g c_{pgas} + k_f c_f}{k_g c_{vgas} + k_f c_f}, \quad \text{where} \quad c_{pgas} = J_0 \, gas/T_0 \quad \text{and} \quad c_{vgas} = J_0 \, gas/T_0 - AR$$

are obtained in the usual way for a flow-type 2, to mouth pressure $p_m = 0$. The T_0 curve at the same time represents the boiling point of BeO, since the combustion temperature is determined by the boiling point of the BeO. For Mg, whose lower heat value is actually negative, the large fraction of liquid-solid phase results in very high temperatures and heat content of the total mass and especially low $\bar{\varkappa}$ values, so that the burning mass rapidly loses the characteristics of a gas or vapor and approaches the behavior of a hot lava.

From the given values of maximum exhaust speed, the resultant effective exhaust speeds for the individual light-metal fuels at 100 atm. furnace pressure can be computed, if we take account of the jet efficiency corresponding to the $\varkappa$ values for $d'/d_m = 0.14$, using the relation

$$\left(\frac{d'}{d_m}\right)^2 = \frac{c}{c_{max}} \cdot \frac{\left(\frac{\varkappa+1}{2}\right)^{\frac{1}{\varkappa-1}} \left(\frac{\varkappa+1}{\varkappa-1}\right)^{\frac{1}{2}} \left(\frac{p_m}{p_0}\right)^{\frac{1}{\varkappa}} \left[1-\left(\frac{p_m}{p_0}\right)^{\frac{\varkappa-1}{\varkappa}}\right]}{1 - \frac{\varkappa+1}{2\varkappa}\left(\frac{p_m}{p_0}\right)^{\frac{\varkappa-1}{\varkappa}}}$$

In first approximation, $\varkappa$ was obtained from the somewhat too large mean value between To and o, instead of between To and T_m; this leads to less favorable values.

BeO :	$\varkappa = 1.20$;	$\sqrt{\eta_D} = c/c_{max} = 0.844$;	c = 3170 m/sec;
B_2O_3 :	1.10;	0.690;	3180 ;
Li_2O :	1.31;	0.925;	3030 ;
Al_2O_3 :	1.24;	0.880;	2670 ;
H_2O :	1.22;	0.865;	3820 ;
MgO :	1.08;	0.630;	2210 ;

(The approximate mean value for $\varkappa$ is 1.255 for octane and gives c = 3120 m/sec. For purposes of uniformity, these numbers were used in later comparison calculations).

For application to rockets, in addition to the effective energy concentration in the mass, the effective concentration E_v in the tank volume is important, since it determines the size of the fuel tanks, rate of feed of the injection pumps and the evaluation number k of the fuel.
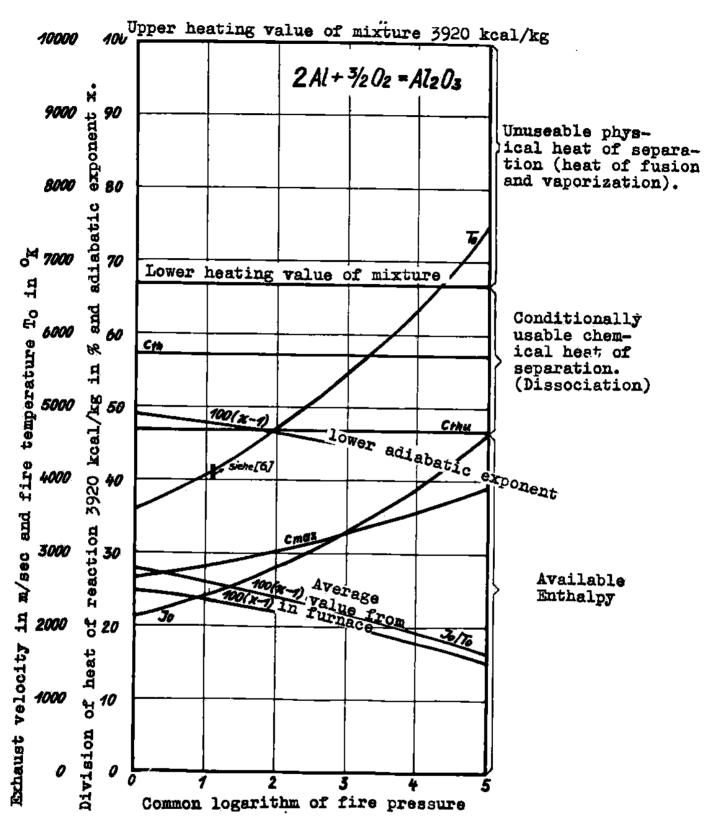
Figure 19: Heat of vaporization, dissociation, heat content, firegas temperature, theoretical and maximum exhaust velocity and adiabatic exponent of firegases for the burning of aluminum in oxygen with static equilibrium.
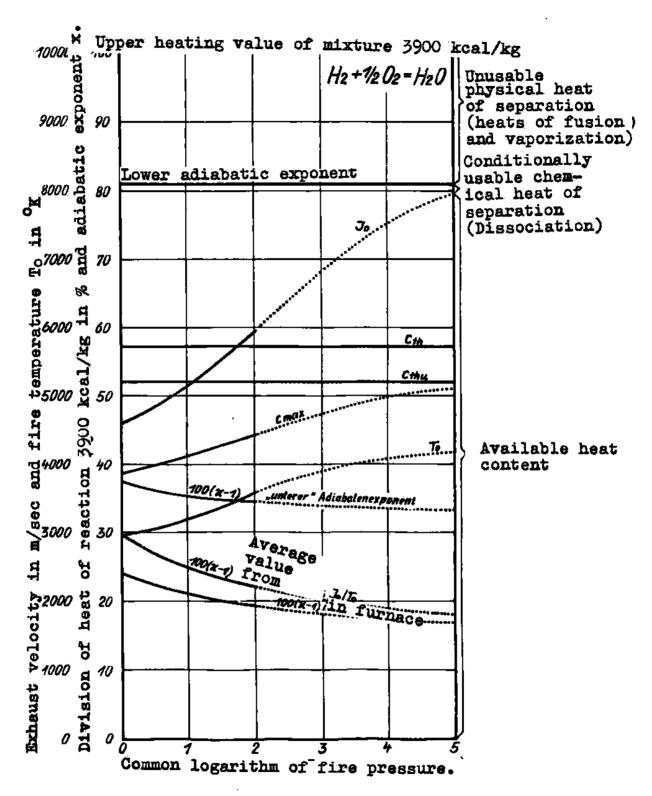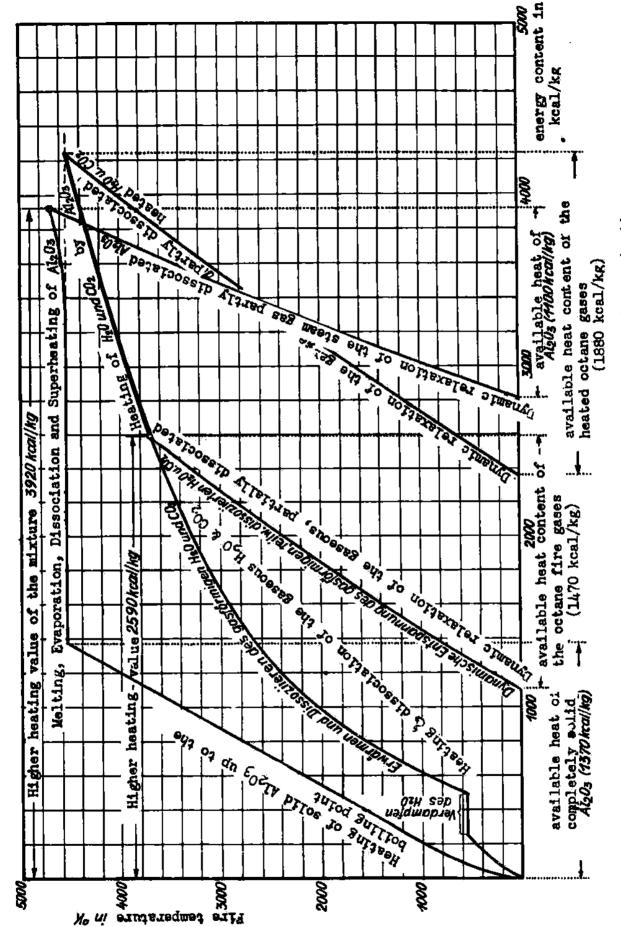
C-84296

Figure 20; Heat of condensation, dissociation, enthalpy, fire-gas temperature, theoretical and maximum exhaust velocity and adiabatic exponent of firegases in the burning of H_2 in O_2 with static equilibrium.

Fig. 21: Energy – Temperature – diagram of aluminum plus hydrocarbon combustion in O_2 at 100 atmospheres chamber pressure and static behavior of the gases.

Beryllium mit Flüssigsauerstoff E_v = 1580 kcal/dm³; K = 1,23;

Bor mit Flüssigsauerstoff   1640   ;   1,27;

Lithium mit Flüssigsauerstoff   820   ;   9,64;

Aluminium mit Flüssigsauerstoff   1390   ;   0,68;

Flüssigwasserstoff mit Flüssig-
sauerstoff   780   ;   1,22;

Magnesium mit Flüssigsauerstoff   840   ;   0,25.

Die Standardwerte fur Oktan (Gasöl)
mit Flüssigsauerstoff betrugen E_v = 1240 kcal/dm³; K = 1,00.
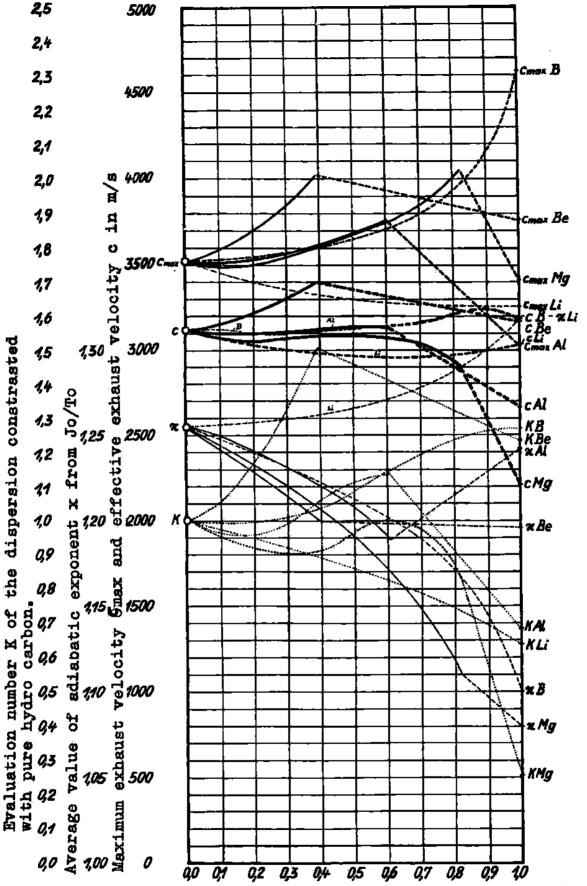
Thus we arrive at the result that, among the fuels in the second group only Be, B and liquid H_2 are superior to hydrocarbons. Be and B are immediately eliminated since, under the conditions possible in the tank, they are in the solid state, so that feeding them into the high pressure furnace of the rocket motor is impossible. If one should try to overcome this difficulty by using the material in the form of wire or powder, then the concentration in the tank would be decreased so much that the calculated small superiority would be lost. Use of fuel in the liquid state is eliminated because of the high melting point. So apparently liquid H_2 is the only material in the second group of fuels which can compete with hydrocarbons. Its 22% superiority is endangered by the fact that at the temperature of liquid H_2, condensation of the surrounding air will start on the metal tanks in the aircaft, so that the rate of evaporation of the H_2 will be increased and the aerodynamic forces will be affected, unless special precautions are taken. Nevertheless, liquid H_2, because of its easy procurement and also for reasons to be discussed later, may be considered as a most promising rocket fuel.

Since, with this exception, the light metals are only slightly (if at all) superior to hydrocarbons as fuel, a second possibility should be tested,- a combination of two e.g. in the form of metallic suspensions in mineral oils. Suspensions not only combine good feed characteristics (they are easily pumped) with high energy density (with consequent low requirements on tank volume and feeding speed); in many cases they have the amazing property that their heat content is greater than that of their individual components such as hydrocarbons and light metals. (30) Fig. 21 shows cycles for Al- O_2 and octane - O_2 at 100 atm. flame pressure. A comparison of these shows the interesting fact that the end temperature in the combustion of octane (3700° K) is about 830° lower than the boiling point of Al_2O_3. If one assumes that equal stöchiometric mixtures of octane -O_2 and Al -O_2 are burned together, that relaxion-free heat exchange takes place between all the molecules of both burning gases, and that finally the two burning masses do not interact appreciably chemically, then one sees from the two cycles that energy will flow from the higher temperature level of the Al_2O_3 to the colder octane. This will be heated at the expense of the heats of dissociation and vaporization of the aluminium combustion gas until the boiling point of Al_2O_3 (4530° K) is reached. After this process of temperature equalization has occurred, the useful heat content of the octane will have risen considerably, while the heat content of the Al gas will not have changed appreciably; i.e., the heat content and maximum exhaust speed of this 70% Al-octane suspension are larger than for Al or octane alone. The advantages of the combination are the following:

1. The temperature of the burning gases for the suspension has not taken on a value midway between those of the individual components, but rather the whole combusting mass has reached the boiling point of Al_2O_3. The requisite energy has been obtained at the expense of the otherwise unavailable energy of dissociation and vaporization of the Al_2O_3.

2. As a result of the temperature equalization between the two fuels in the suspension, the relatively slight dissociation of Al_2O_3 has been decreased, while that of the octane has increased markedly. Thus the average specific heat c_p = J_0/T_0 of the gas has increased, as one can see from the smaller slope of the expansion curve for the octane. Both these circumstances result in increased heat content J = c_pT.

One realizes, moreover, that the random example of a 70% suspension chosen here, which has equal parts by weight of Al - and octane - combustion gases, may not give the best results for c_{max}. The best Al - octane suspension will be one having enough Al to heat the entire mass to the boiling point of Al_2O_3. The upper heat values of the Al will be fully used in this case, since no metallic oxide vaporizes. The extra heat of vaporization and dissociation of Al_2O_3 are used to increase the heat content and dissociation of the octane. The best results are obtained for a 60.5% Al - octane suspension.

The considerations concerning the Al - octane suspension can be extended to the other light metals. Fig. 22 shows for Be, B, Li, Al and Mg suspensions with varying metal content, the chief

40

Figure 22; Properties of the metal oil dispersions against metal
content at 100 atmos chamber pressure.

41

characteristics of the combustion at 100 atm furnace pressure: maximum exhaust speed, average adiabat exponent, effective exhaust speed in flight, and evaluation number K. From the graph we see that those fuels, like B and Li, the boiling point of whose oxide is below the end temperature of combustion of octane, do not show the characteristic effect of the dispersion. For them the curves of C_{max}, $\varkappa$, and c, show no maximum; i.e., the suspension is no more favorable than the better of its two components. For the remaining materials, Be, Al, and Mg, the characteristics at optimum composition are:

for Be - hydrocarbon fuel with 39% by weight of metal C_{max} = 4100 $m/_{sec}$, $\varkappa$ = 1.20; c = 3400 $m/_{sec}$; K = 1.51; E = 1557 $\frac{kcal}{dm^3}$

for Al - hydrocarbon fuel with 60.5% by weight of metal C_{max} = 3760 $m/_{sec}$; $\varkappa$ = 1.189; c = 3140 $m/_{sec}$; K = 1.14; E = 1453 $\frac{kcal}{dm^3}$

for Mg - hydrocarbon fuel with 80% by weight of metal C_{max} = 3725 $m/_{sec}$; $\varkappa$ = 1.171; c = 3080 $m/_{sec}$; K = 1.00; E = 1330 $\frac{kcal}{dm^3}$

Summarizing we can say: Mg dispersed in hydrocarbon has no advantages over pure hydrocarbon. Al and Be show a wide range of suspensions in which they are superior to the pure hydrocarbon by up to 14% and 51% resp. Because they are easily obtained, Al - suspensions have special importance for military rocket-flight technique, while Be - suspensions come into consideration for special uses. All the studies were limited to stöchiometric proportions, so the possibility still exists that other mixture proportions may reach better values of K or c.

The preparation of 60% Al - gas oil suspensions, which are still usable after many weeks if left untouched, and which are easily fed through centrifugal pumps, was done in two ways on the basis of suggestions by H. Troitzsch and E. Russer:

1. Increasing the viscosity of the gasoil by dissolving various materials such as metallic salts of fatty acids, waxes, fats, rubber or various synthetics. Good results were obtained in tests with natural and synthetic rubber, and similar high-polymer hydrocarbons, the oppanols. The oppanols have the further advantage that, being pure hydrocarbons, they require no ballast materials, but burn completely with large heat output.

2. Decrease of particle size of the Al dust while hindering surface oxidation as much as possible, since with decreasing particle size, the sedimentation speed and, in most cases, the viscosity decreases. (?) For these large quantities of metal, pulverizing by using supersonics seemed impractical. So the powder was ground in ball-mills in a nitrogen atmosphere.

In connection with the use of liquid O_2 as a component of all the rocket fuels discussed so far, the problem of storing very large quantities of this material is important. Because its boiling point is - 183° C, it will be continuously boiling as a result of the steady flow of heat from its warmer surroundings, and will liberate the energy absorbed by vaporizing with a heat of vaporization of 51 kcal/kg, so that the residual material can maintain itself at this low temperature. This undesirable vaporization can be decreased by lowering the heat transfer from the surroundings, which occurs mainly through the tank walls which are wet by the liquid. A first method is the decrease of the wetted surface by putting all the material to be stored into a single tank of spherical shape. The heat flow through this smallest surface can be further decreased by the use of various standard heat-insulation procedures, of which heat-stopping materials like loose powder of magnesium carbonate, with a heat conductivity of λ = 0.027 kcal/mh°, have shown themselves effective, in the form of thick layers. In the existing temperature range of + 20°C to -183°C, 131 kcal per square meter of tank surface will go through a 1 meter thick insulating layer during a 24-hour period; this corresponds to O_2-vaporization at the rate of 2.57 kg per day per sq. meter of surface. With these figures, the daily loss by vaporization is shown in Fig. 23, for various containers up to a million ton capacity, for three thicknesses of the insulating layer 1m, 5m, and 10m, and taking account of the spatial heat flow through the thick walls.

The results of this calculation were confirmed in a trial installation of a liquid O_2 tank with 56 ton capacity and a magnesium carbonate insulating layer of average thickness 2.6m. This tank has been running at the aircraft-testing station at Trau since 1938; the manufacturer is the " Aktiengesellschaft für Industriegasverwertung Berlin - Britz". Although even this tank, (though small as measured by rocket-technical requirements) represents a brand-new development as compared to all previously constructed liquid O_2 containers, and no experience with tanks of such size existed, the tank worked satisfactorily from the first day it was used. Its vaporization is 140 kg/day, which is exactly the theoretically expected value, as can be seen by substituting the
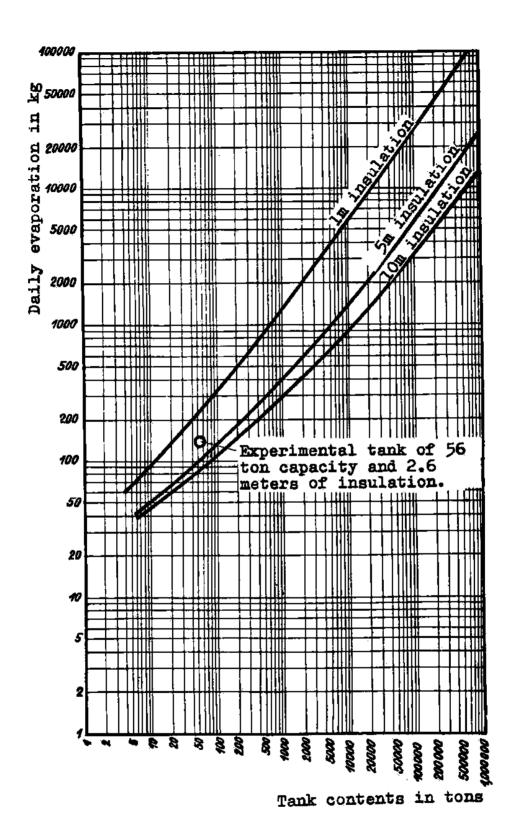
Figure 23; Daily evaporation loss from cylindrical large scale containers for liq. O_2 for various capacities and various thicknesses of inorganic insulating material.

tank-volume, insulation thickness, daily vaporization in Fig. 23. In the photograph, Fig. 24, can be seen the 8 m. high, 8m. diameter outside cover of the tank. Inside this steel cover hangs the actual container for the fluid; it is made of brass and has a capacity of 50 m³ or 56 tons. The space between the two metal shells averages 2.6 m in width, and is loosely filled with finely powdered magnesium carbonate. The whole tank stands freely in a subterranean space, where it can be approached and examined from all sides. This room has a completely normal cellar climate; no noticeable drop in temperature can be observed. The outer steel cover of the tank is also at normal temperature; moisture in the air does not condense on it. The 140 kg. of O_2 vaporized each day are collected in flasks and are used for operation of the testing station and for welding.

Fig. 25 shows a schematic diagram of a large container for a million tons of liquid, which has a daily evaporation of 13,000 kg. for a 10 m. insulation thickness. This container, when once filled and left alone, will become empty only after 200 years. The amount evaporated daily can be used by simply filling steel flasks and transferring them to the consumer. The cylindrical inner container of Cu-alloy has a diameter of 103.5 meters. and, including the arched base, a height of 119 m. The bottom end is conceived of as a hanging floor which rests on a ring running along the boundary of the outer cylinder. This ring is supported on the ground by poorly conducting pillars placed at intervals. The top cover is hung on the outer steel cover at various points. The insulating layer of loose magnesium carbonate powder is around the inner container, and is 10 m. thick on the sides and cover, 15 m. thick below the floor. This insulating layer is bounded and supported by the steel cover which is rigid and strong. The whole thick-walled container stands on a cylindrical subterranean bunker of reinforced concrete.

The liquid O_2 comes in through the intake at the left and is led through the intake pipe to the floor of the container, in order to excite as little motion of the oxygen during filling as possible. At the top of the tank is the drain pipe for the vaporized gaseous O_2, by means of which normal atmospheric pressure is maintained above the liquid surface. The liquid is removed at the lowest point of the container. At the same level as this point, a pump system stands on the right at the edge of the bunker, and feeds the liquid to the outlet at the top edge of the bunker.

Further details and auxiliary equipment of the tank will not be mentioned here, but the behavior of the liquid O_2 in the large tank requires further consideration. In the liquid pool, which has a depth up to 117 meters, the hydrostatic pressure, as shown in Fig. 25, increases with the depth up to 13.1 atm. The boiling point of O_2 depends on the pressure, and increases with depth in the liquid from -183° C at 1 atm to -144° C at 14.1 atm. In spite of this, the entire contents of the tank will stay at -183° C, the temperature of the surface of the liquid. For if the masses of liquid down below should warm to higher temperatures than the upper layers, their density would decrease and a convection would occur which brings the warmer masses upward to the region of lower hydrostatic pressures, where as a result of the decreased pressure they will begin to boil, give off the heat of vaporization of the liberated gas, and cool to the temperature of their surroundings. Since this process holds for layers at any depth, the lowest temperature at the liquid surface will bring all the lower layers to the same temperature. Thus in practice one will actually find the liquid at the bottom of the tank to be at -183° C. Since the heating occurs mainly through the side walls, the movement of the fluid will be such that the heated boiling masses of liquid rise along the walls, while the cold masses sink in the middle of the tank so that the toroidal streaming shown in Fig. 25 develops.

Liquid O_2, whose combustion properties and storage have been discussed in detail here, need not give, in combination with the previously described fuels, the greatest exhaust speed. Therefore, two further notable candidates will be discussed briefly - fluorine and ozone (or ozone-enriched liquid O_2).

Fluorine would be used only for metallic fuels. The corresponding metal fluorides in some cases have higher heats of formation and lower heats of vaporization than the oxides, give the prospect of higher exhaust speeds, but are not considered further because of the technical difficulties in using liquid fluorine in place of liquid O_2. The use of pure ozone can be easily checked for the case of octane. Since ozone has available a disintegration energy of 710 $\frac{kcal}{kg}$, the heat-output of the mixture increases from 2587 $\frac{kcal}{kg}$ for O_2 to 3140 $\frac{kcal}{kg}$ for ozone, and the theoretical exhaust speed c_{th} = 4655 m/$_{sec}$ increases by 10% to 5120 m/$_{sec}$. The use of pure ozone increases the effective exhaust speed by this same order of magnitude.

To test the applicability of ozone to rockets, H. Schumacher in Frankfurt made tests on a small scale, with the following main results:

Both gaseous and liquid pure ozone are explosive under the working conditions in flight, and are thus not suitable. Gaseous ozone - O_2 mixtures at N.T.P. will react, in pipes or spherical chambers, starting at a 10% weight fraction of ozone, if the reaction is initiated by an
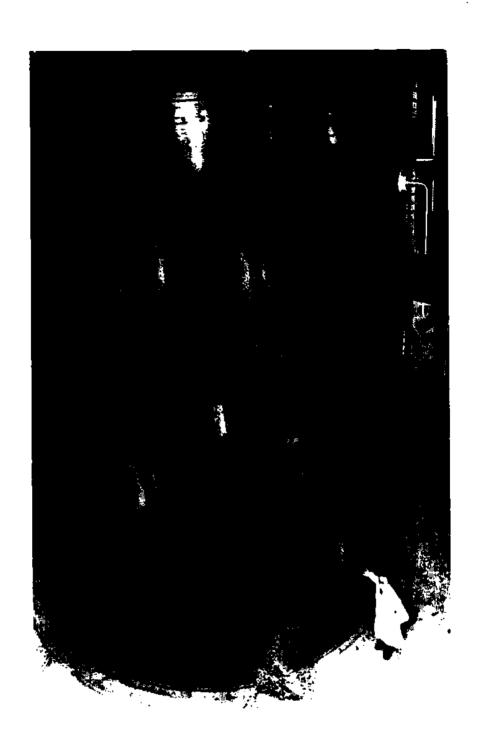
44

Figure 24; External view of liq. O_2 tank of 56 ton
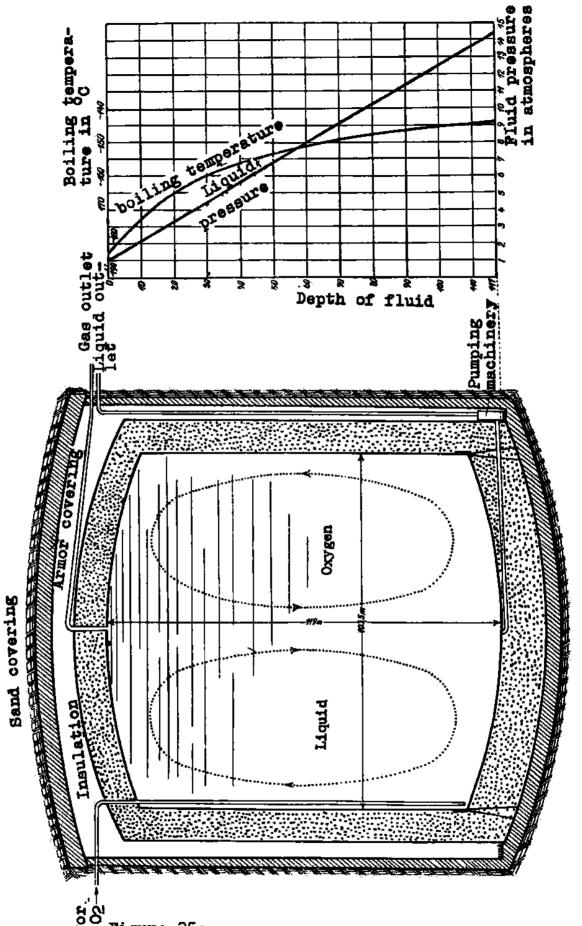capacity, 2.6 m insulation thickness and
140 kg daily evaporation.

Figure 25;
Sketch of an enormous tank for 1 million tons of liq. O_2
with a diagram of the pressure and boiling point ratio
in the liquid content.

incandescent body, but the reaction will not spread to all of the mass until the ozone concentration reaches 17% by weight. Even then the pressures developed in the reaction are so moderate that they might be expected to require motors and armatures.(?) The pressure increases are of the order of 2 atm. A luminosity starts only at ozone concentrations of 40-50% by weight, and the pressure increases reach 6-10 atm.

Liquid ozone-oxygen mixtures at atmospheric pressure and the corresponding boiling point seem to have, for weight % of ozone above 25%, a tendency to explode with great destructive effect, if gaseous ozone above them explodes with emission of light. The miscibility of liquid ozone with liquid O_2 and the boiling point of the mixture are sufficiently understood from the solubility diagram and vaporization curve at atmospheric pressure, that we assume the following regarding the storage of large quantities of the mixture in open containers:

Mixtures up to 25% by weight of ozone are stable, do not separate, and have a temperature of -183° C. Since such mixtures seem to be safe from explosion, they are of importance for technical use. Mixtures between 25 and 55 weight % of ozone are not stable; they split into a heavier, deep violet, ozone-enriched phase (>55% O_3), which sinks to the bottom, and a lighter, light blue, O_2-enriched phase (>75% O_2), which floats above. The phase which sinks is probably explosive. Mixtures with more than 55% ozone by weight are again stable but in danger of exploding, so they are without immediate technical value.

For increased pressures the critical solubility temperature of -179.5 is quickly passed, and a miscibility gap no longer occurs. Liquid ozone-liquid oxygen mixtures which are stored for long periods become ozone-enriched because of the more rapid boiling off of O_2, so that the resultant explosive tendency of the tank contents must be counteracted by adding O_2. The gas phase above the liquid surface reaches the critical ozone concentration of 40-50 weight -% only for ozone concentrations >90% in the liquid phase, so that the products of vaporization of liquid ozone - O_2 mixtures of up to 25% ozone content are scarcely dangerous even for rapid vaporization on uncooled machine parts. Fig. 26 shows the behavior of liquid ozone-liquid O_2 solutions.

A few other oxidizing agents are mentioned in the first part of this book; two of them, H_2O_2 and HNO_3 have attained some practical value for certain rocket uses.

Aside from the three groups of non-self-acting rocket fuels : combustion of hydrocarbons with O_2 or ozone, burning of light metals in O_2 or fluorine, and the combination of the two groups in the form of light metal-hydrocarbon suspensions, a fourth group of self-acting fuels is possible, which use the heat liberated in formation of molecules from the substance in atomic form: atomic nitrogen (9)   (11)

$$2N = N_2 + 6050 \; kcal/kg \quad , \quad c_{th} = 7120 \; m/sec$$

and atomic hydrogen

$$2H = H_2 + 51400 \; kcal/kg \; (11,32), \quad c_{th} = 20,800 \; m/sec$$

Since the life times of these unstable materials is very short (the life time of active hydrogen is given as at most 10 sec [9, page 253], research in this branch of rocket fuel development must first take the following lines: 1. Finding a basic method for prolonging the life of active nitrogen or hydrogen. 2. Determination of the dependence of lifetime on temperature and pressure, especially in the direction of very low temperature. 3. If necessary, development of a method for enriching liquid or solid material with the monatomic modification.

Though the difficulties of such research may be great, and the prospects of technically valuable results are small, it should be noted that, because of the 10-20 times greater energy concentration of H as compared to presently available fuels, the more favorable specific heat, the higher æ values - i.e., greater jet efficiency, the higher reaction velocity - i.e., greater furnace efficiency for smaller furnace volume, and the highly diathermic behavior - i.e., slight thermal stress on the furnace walls; even partial successes, say a 10% enrichment of H in H_2 by perhaps dissolving gaseous H in liquid H_2, would be of extraordinary technical importance. For the limiting case of 100% N or H concentration as starting fuel for combustion, the following characteristic quantities were calculated for a furnace pressure of 100 atm:

$$N_2: T_o = 8260° \quad ;æ = 1.49; \quad \sqrt{\tfrac{}{}} = 0.97; \quad c = 4690 \; m/sec$$

$$H_2: T_o = 5500° \quad ;æ = 1.49; \quad \sqrt{\tfrac{}{}} = 0.97; \quad c = 14100 \; m/sec$$

For atomic hydrogen these values are plotted in Fig. 27 for various flame pressures. This diagram shows clearly the extraordinary properties of active hydrogen; i.e., that the probability of regaining large portions of the dissociation energy by after-burning in the jet is very large.
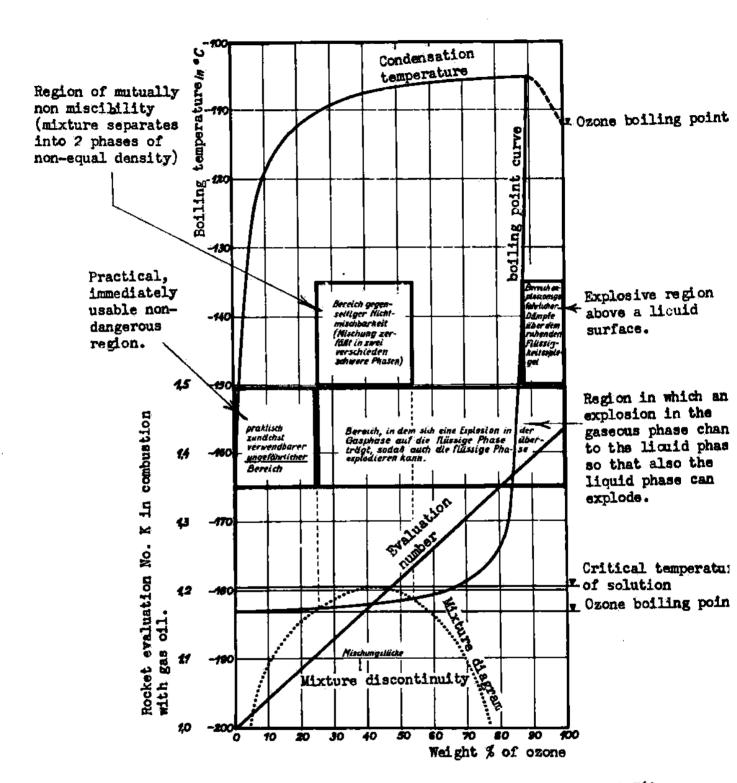
Region of mutually non miscibility (mixture separates into 2 phases of non-equal density)

Practical, immediately usable non-dangerous region.

Boiling temperature in °C

Condensation temperature

boiling point curve

Ozone boiling point

Explosive region above a licuid surface.

Region in which an explosion in the gaseous phase chan to the licuid phas so that also the liquid phase can explode.

Bereich gegenseitiger Nichtmischbarkeit (Mischung zerfällt in zwei verschieden schwere Phasen)

Bereich, in dem sich eine Explosion in Gasphase auf die flüssige Phase trägt, sodaß auch die flüssige Phase explodieren kann.

der über-se

praklisch zundichst verwendbarer ungefährlicher Bereich

Rocket evaluation No. K in combustion with gas oil.

Evaluation number

Critical temperatu of solution
Ozone boiling poin

Mixture diagram

Mischungslücke

Mixture discontinuity

Weight % of ozone

Fig. 26: Behavior of mixture of liquid ozone and liquid oxygen at 760 mm pressure according to Schumacher-Frankfurt.

48

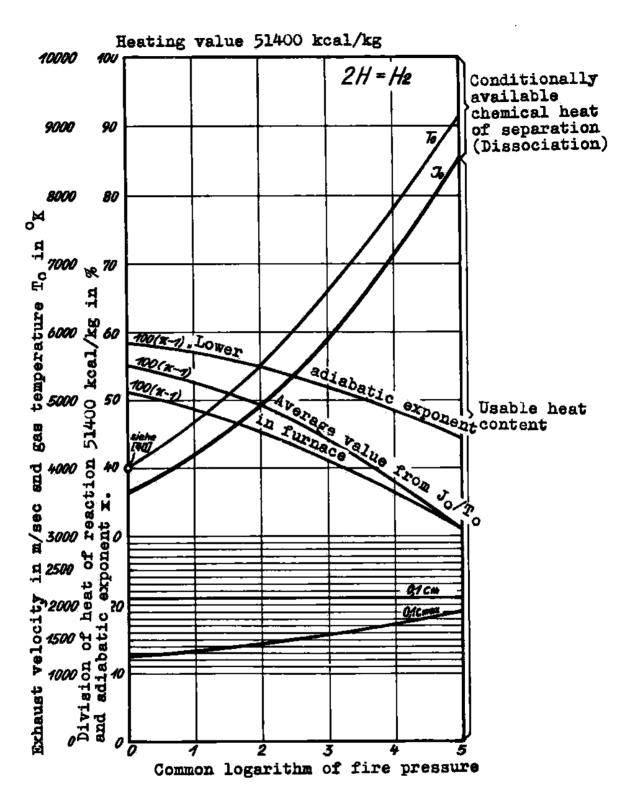Heating value 51400 kcal/kg

$2H = H_2$

Conditionally
available
chemical heat
of separation
(Dissociation)

T_o

J_o

100(κ-1) Lower
100(κ-1)
100(κ-1)

adiabatic exponent

Usable heat
content

siehe
[40]

Average value
in furnace
from J_o/T_o

J_o/T_o

0,1 см

0,1 см

Common logarithm of fire pressure

Exhaust velocity in m/sec and gas temperature T_o in °K

Division of heat of reaction 51400 kcal/kg in % and adiabatic exponent κ.

10000 100
9000 90
8000 80
7000 70
6000 60
5000 50
4000 40
3000 0
2500
2000 20
1500
1000 10
0   0

0   1   2   3   4   5

Figure 27; Dissociation, heat content, combustion temperature,
theoretical and maximum exhaust velocity and adia-
batic exponents for fire gases in the case of assoc-
iation of active H2 to molecular H2 with static
equilibrium.

49

C-84296

Finally another group of fuels is worthy of note: These fuels based on nuclear reactions can result in exhaust speeds of 10^6-10^8 m/sec, and have recently, because of the reactions in uranium fission, moved into the domain of technical interest. (3).
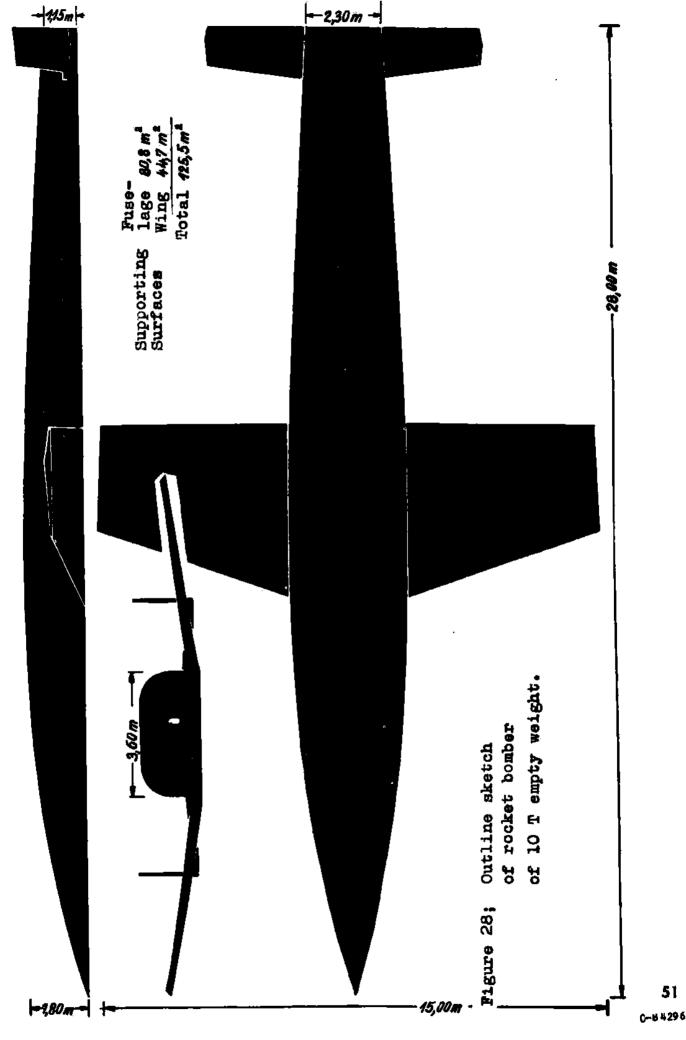
Summarizing the numerical results of this section concerning the problem of exhaust speeds, we may say that by means of stochiometric combustion of hydrocarbons in O_2 in rocket motors at 100 atm. furnace pressure, exhaust speeds above $c = 3100$ m/sec are possible. For excess fuel, 5% higher values are obtained. By enriching the O_2 with ozone, a further increase of exhaust speed to $c = 3400$ m/sec may be possible with stochiometric mixtures. The use of Al - hydrocarbon suspensions with liquid O_2 gives similar exhaust speeds, but more favorable proportions by weight on the aircraft, because of the higher fuel density. We may expect exhaust speeds, of rocket motors in flight, over 3800 m/sec for liquid H_2 with liquid O_2, and over 4000 m/sec if ozone is included, while the addition of atomic hydrogen would give even higher values. For calculations of flight - and military performance of the rocket bomber we shall use the values $c = 3000$ m/sec, and $c = 4000$ m/sec. To see the effects of higher exhaust speeds we shall calculate with $c = 5000$ m/sec for comparison.

3. Properties of the Air-Frame

The external appearance of the rocket bomber is shown in Figs. 28-31 and discussed theoretically in the next section. The bow of the aircraft's fuselage consists of an "ogival" with 9.6 caliber radius of curvature, which is cut by a plane through its long axis so that a flat underside results for the fuselage. Between the wings the semi-ogive goes over into a roomy chamber with perpendicular side walls, while the fuselage gradually tapers toward the stern with a steady decrease in cross-section. The large blunt end surface at the stern of the fuselage is necessitated by the size of the mouth of the jet of the rocket motor. The relatively small wing stumps serve mainly for stabilization in flight, and for landing; the wing cross-section is the well-known triangular wedge profile with a maximum thickness of 1/20 of the depth at 2/3 of the wing depth. (18, p. 170). To this peculiar aircraft shape there correspond the laws of flow for very high Mach numbers. An angle of incidence between fuselage and wings is unnecessary, so that for the low-wing arrangement chosen, the lifting flat surfaces of the fuselage and wings go over into each other without a break, as can be seen most clearly in Fig. 31. For the tail surfaces, a symmetrical quadrangular cross-section was chosen, which also has a greatest thickness of 1/20 of its depth in the last third of its depth. The whole arrangement of the tail surfaces is independent of the streaming from the rocket jet, since use of the rocket motor and flight below sound velocity never occur together.

The size of the rocket bomber was chosen as a compromise between a series of contradictory requirements. The idea of making the aircraft as large as possible is suggested by the fact that then the ratio of additional load to weight when empty is generally more favorable, that the construction of larger rocket motors is simpler, that with increased size of aircraft the military strength of a rocket bomber group increases while the number of capable pilots required per unit of load transported decreases. If one computes a few comparison designs in the range of 10-100 tons starting-weight, one finds that with increasing weight of the aircraft, the aerodynamical lifting power contributed by the fuselage represents (for geometrical reasons) a smaller part of the total weight, so that the wings have to be relatively larger; finally the weight of the wings predominates, without giving any noticeable improvement in gliding angle in the region of high Mach numbers. Such considerations lead to an apparently favorable takeoff weight of 100 tons, to which corresponds an empty-weight on landing of 10 tons. Thus a limit of 90 tons of fuel with about 76 m^3 tank space must be included, which leads to the fuselage dimensions shown in Fig. 28.

The wing dimensions are determined by the permissible wing loading of the bomber. The starting procedure by rocket catapult, which has already been described briefly, permits practically high wing-loading; thus even though before landing the consumption of all fuel and removal of all ballast reduces the weight to 1/10 the takeoff weight, the landing speed determines the wing size. Though landing speeds of over 200 km/hr can be used in special cases, a permissible limit of 150 km/hr was first chosen because the landing of the rocket bomber is to be considered a glide-landing, and because one cannot count on the availability of experienced test pilots. The corresponding stagnation pressure is $q = 110$ kg/m^2. From Fig. 34, the very thin and slightly curved wing profile leads one to expect a maximum lift coefficient of only $C_{a\ max} = 1.25$ even with landing aids, so that the wing-loading before landing is limited to $q\ C_{a\ max} = 137.5$ kg/m^2. Aside from this figure, the wing size is determined by the fact that the fuselage plays an important role in the lifting power of the whole aircraft. According to the investigations of the next section, for large Mach numbers 2/3 of the total weight is carried by the fuselage, and 1/3 by the wings. At landing speed, the lift coefficient of the fuselage, at the angle of attack for maximum lift, is $C_a = 0.45$; with the already fixed fuselage supporting surface $F_r = 80.8$ m^2 the total lifting power is $F_r \cdot C_a \cdot q = 4000$ kg, while the residual landing weight of 6000 kg goes

Supporting Surfaces	Fuselage	80,8 m^2
	Wing	44,7 m^2
	Total	125,5 m^2

Figure 28: Outline sketch of rocket bomber of 10 T empty weight.

1,15m

2,30m

28,00m
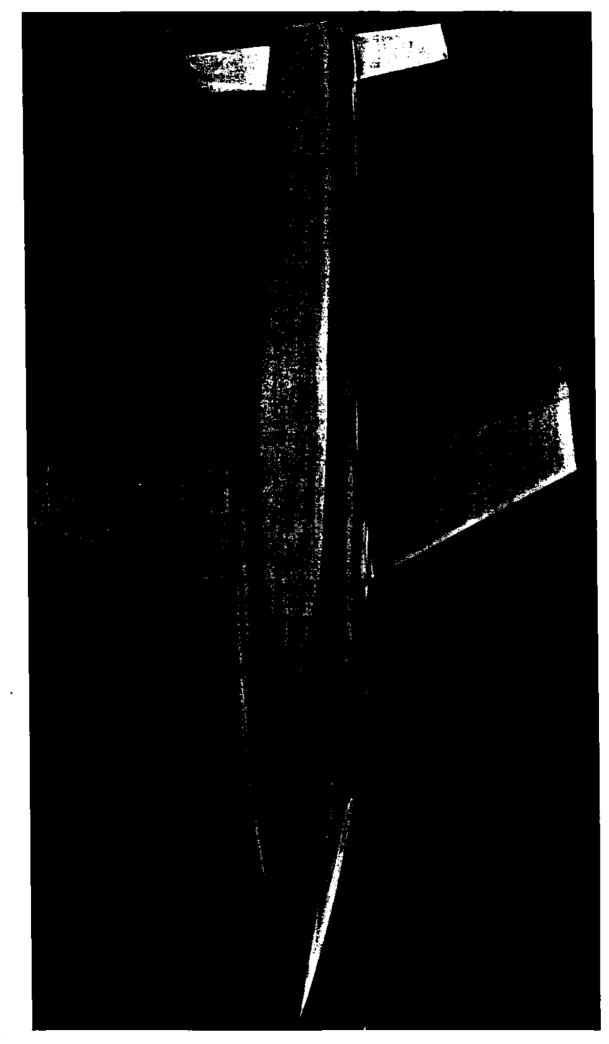
3,60m

1,80m

15,00m

C-84296

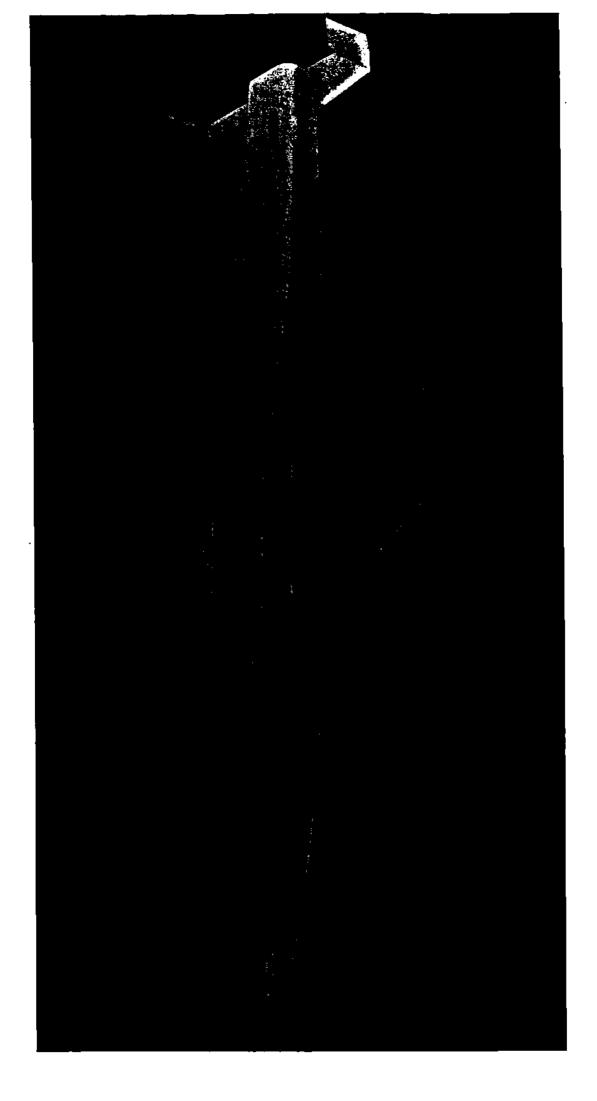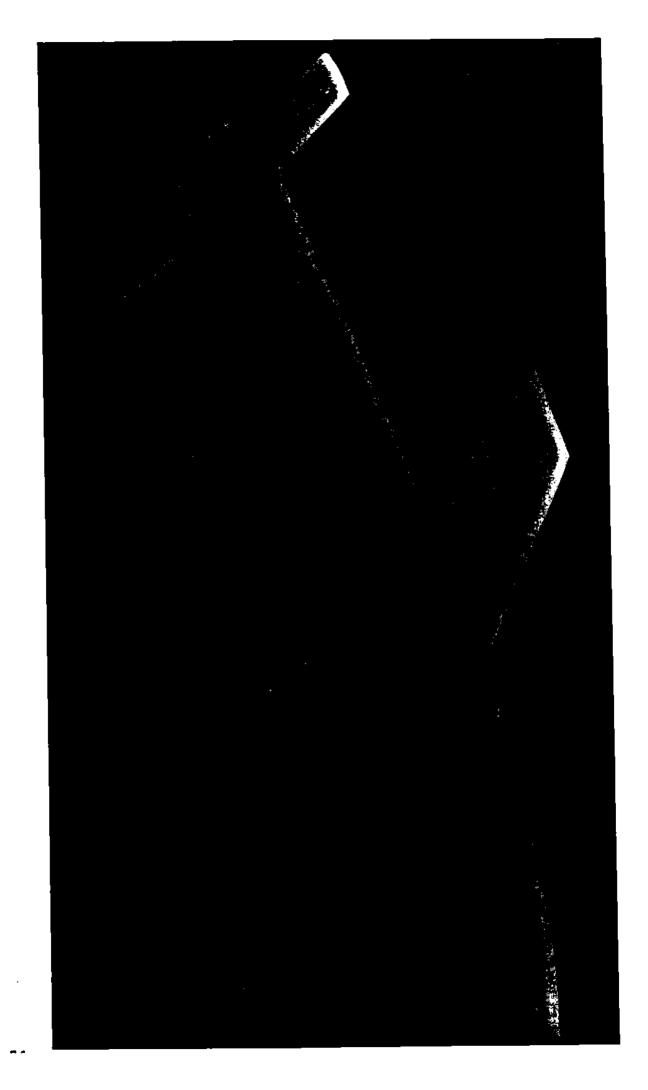Fig. 29: Top view of rocket bomber of 10 ton empty weight.

Fig. 30: Outer form of Rocket Bomber of 10 tons empty weight, perspective view from front-above.

Fig. 31: Perspective view from "backwards below" of 10 ton empty weight Rocket bomber.

to the wings. Thus the required wing size is about 44 m^2; according to Fig. 28, the total supporting surface is 125.5 m^2; the mean wing-loading is 10,000/125.5 = 79.7 kg/m^2 and the lift coefficient for landing is C_a = A/qF = 0.74, in agreement with Fig. 34.
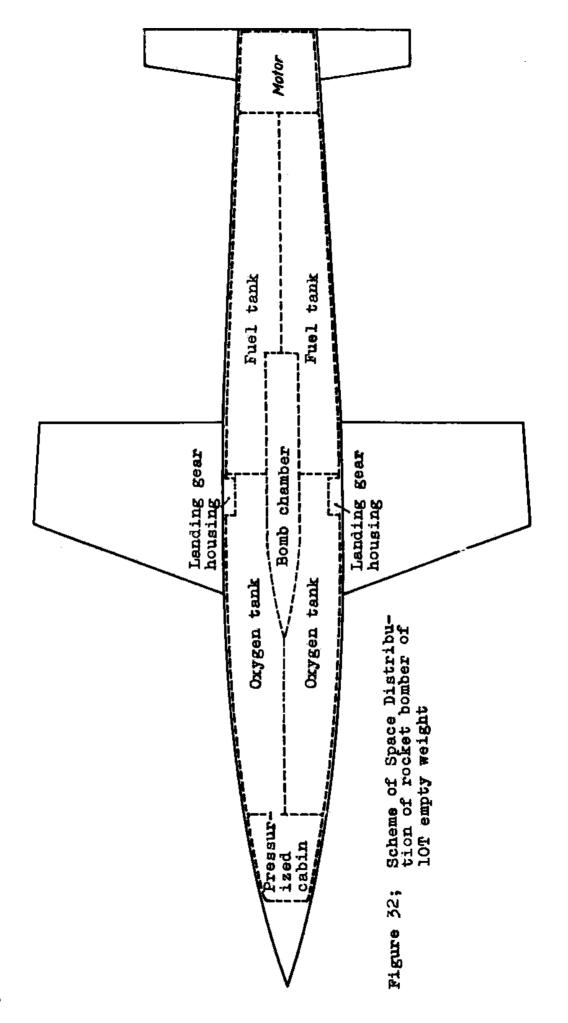
At take off, the mean wing-loading is ten times as high, i.e., 797 kg/m^2; for the assumed climbing speed of 500 m/$_{sec}$ the stagnation pressure at takeoff is 15930 kg/m^2 and the total lift coefficient C_a is 0.05, corresponding to an angle of attack α = 3°, while the lift coefficient at optimum gliding angle is C_a = 0.173 for v/$_A$ = 1.5. At a 3° angle of attack, 38% of the total weight of 10^5 kg falls on the fuselage, and 62% on the wings; the wing loading is thus 1390 kg/m^2. After the aircraft rises to the optimum angle of attack of 8°, C_a becomes 0.173; thus the lift for hauling the craft at V/$_a$ = 1.5 is 346000 kg, of which 48% rests on the wings with C_{aF} = 0.083, corresponding to a wing loading of 3720 kg/m^2 in this state of flight which determines the wing stress.

Other cases of loading are important for various parts of the rocket bomber; e.g., for the fuel tanks it is the acceleration at takeoff; for fuselage and pilot it is the acceleration at the end of the climb; for fuselage and landing gear it is the landing which is important.

In estimating the ratio of empty-weight G, after consumption of all fuel and dropping of the useful load, to the flight weight G$_\bullet$ immediately after rising from the ground, we started from the known weight distribution for overloaded long range aircraft: airframe 18%, power plant 13%, auxiliaries 3%, additional load 66%, so G/$_{Go}$ = 0.34. The main parts of the rocket bomber were estimated as: cabin - 500 kg, rocket motor - 2500 kg, wings - 2500 kg, a total of 56 kg/m^2; fuselage 3250 kg, tail, landing gear, bomb-bay, etc., altogether 1250 kg; thus the total weight of the aircraft is 7000 kg, whereas flight weights for ordinary bombers of similar size are about 3000 kg. The reason that the rocket bomber with its 10 times greater takeoff weight is only 2.3 times as heavy as an ordinary bomber of the same size is mainly because the supporting surfaces, especially the wings, carry not 10 times but only 3-4 times the weight, while the remainder is directly supported by the air without any intermediary structure; moreover because of the definite way of starting and climbing the factor of safety for the rocket bomber need be only a small fraction of that for an ordinary bomber. Thus the total weight distribution f the rocket bomber is airframe 7%, power plant 2.5%, auxiliaries 0.5%, additional load 90%, so G/$_{Go}$ = 0.1. All these considerations are valid for scaled-up weights. One thus obtains directly the correct performance figures, if the bomb load is diminished by the excess weight, above 10 tons, of the aircraft.

Figs. 32 and 33 show an overall schematic of the rocket bomber.

The front view of the craft does not show the retractable front wheel, which operates in conjunction with a retractable tail skid and the landing gear which is retractable into the fuselage between the wings. The front wheel serves to prevent dangerous contact with the ground of the bow end during the bouncing motion of the aircraft during landing, and to slow down (with the aid of the landing gear) as quickly as possible the aircraft which comes on to the ground at 150 km/hr and has practically no wind resistance then because of the small wings. Behind the bow is the pressure-tight cabin, in which the single pilot sits. It is tight for inside pressures of 0.4-0.5 atm. with vacuum outside, and should permit rapid exit of the pilot in case of danger (e.g. after takeoff). Because of the smooth external shape, visibility from the cabin is very poor. In free flight at high velocity, side view slits and optical aids are sufficient. For landing a kind of detachable windshield can be used, since than the pressurization of the cabin and maintenance of the bullet-shape are unimportant. A further essential arrangement for the cabin is that the pilot's seat be so arranged that the pilot can take up the high accelerations along the aircraft axis in the best possible position, so that not only body and head, but also feet and arms have good supporting surfaces, and at the same position can be shifted. The remaining equipment of the pilot's cabin - instruments, D/F and radio equipment, ventilation, etc. is not considered further. At the back of the pressurized cabin are the tank installations, which consist of two large tubes 20.5 m. long and with maximum diameter 1.8 m; these constitute the main part of the fuselage. The upper fourth of the tubes' circumference forms the skin of the aircraft, while the lower half and the space between the tubes is covered so that the required shape is obtained. For constructional reasons the tank tubes are subdivided into the actual containers by means of cross-walls. The purpose of the cross-walls is first to have separate containers of correct capacity one behind the other for fuel and liquid O_2 and that each fuel shall lie symmetrically with respect to the axis of the aircraft, so that thermal stresses and twists are not developed due to asymmetries; second, as a result of the subdivision, to lower the liquid pressure on the rear end of the tank during acceleration and to prevent the aircraft from becoming tail-heavy as the tanks are emptied; finally the cross walls give the thin-walled fuselage the stiffness necessary for taking up the torques at the roots of the wing-spars. It is advisable to put the oxygen tanks in the front end of the fuselage so that the force driving the O_2 to the
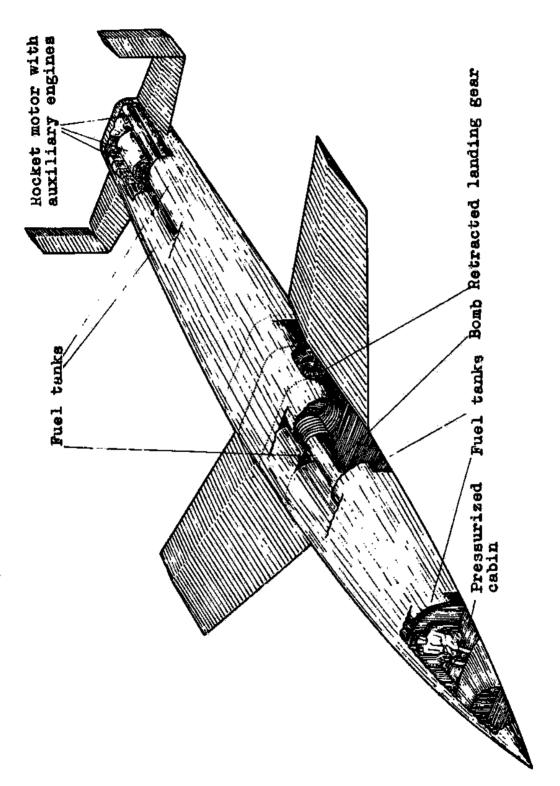
55

Figure 32: Scheme of Space Distribution of rocket bomber of 10T empty weight

C-84296

Figure 33: Total view of 10 ton Rocker Bomber

Rocket motor with auxiliary engines

Fuel tanks

Pressurized cabin

Fuel tanks

Bomb

Retracted landing gear

pumps will be as large as possible. Between the wings and the tanks is the bomb bay, suitable for projectiles up to 30 tons in weight. When the bombs are released, the floor of the bomb bay must be opened completely for a short time so that the axis of the bomb is parallel to that of the aircraft, since in the perpendicular position premature detonation may occur. Just before the main spar meets the fuselage there are chambers for the extendable landing wheels; these chambers are partly on the vertical sidewalls of the fuselage and partly recessed into the tank cylinders.

Finally, Fig. 33 shows the rocket motor at the end of the fuselage.

4. The Glide-Number of the Air-Frame

During its flight the rocket bomber goes through velocity ranges with entirely different flow characteristics, e.g., the ordinary subsonic range, the supersonic range up to three times the velocity of sound, the domain of large Mach numbers V/a, in which Newton's law of air resistance is valid - i.e., the aerodynamic forces vary with the square of the velocity and the angle of attack; and finally the range of gas-kinetic streaming with very long free paths of the air molecules and thus special laws of air resistance which are still similar to Newton's.

In all these regions the aircraft must have sufficient stability characteristics, whereas the glide-angle is important chiefly in the Newtonian region for both density types, for if the rocket bomber at the beginning of its glide had Mach number 30, then 99% of its kinetic energy, would be consumed in the Newtonian region, and only 1% below a Mach number of 3.

In the region of higher densities the glide angle can be estimated at only a few special points on the Mach scale, say $V/a = 0.1$; 1.5; 3 and ∞, whereas for rarefied air closed gas-kinetic formulae can be given.

For a landing speed of 150 km/hr, i.e., $V/a = 0.12$, polars of the bomber and the wings were determined by wind tunnel tests on a 1:20 scale model; the results are shown in Fig. 34. The best reciprocal glide number is $1/\epsilon = 7.75$ for angle of attack $\alpha=5°$; the best lift coefficient is $C_{a\ max} = 0.575$ for $\alpha=16.5°$.

For V/a between 1 and 3 the difference in pressure compared to the pressure of still air is, for two-dimensional flow at small angles of attack,

$$\Delta p/q = \pm 2\alpha/\sqrt{V^2/a^2 - 1},$$

according to Ackeret and Busemann; for spatial flow around the rotation-symmetric end of a cone

$$\Delta p/q = 2\alpha^2 \ln[(2 \ tg \ arc \ sin \ \alpha)/\alpha]$$

according to Busemann and V. Kármán, and the tangential friction stresses are $\tau/q = 0.072 \left(\frac{1}{Re}\right)^{0.2}$ according to V. Kármán. With the aid of these relations the values given in Fig. 35 and 35, for polars of the wings, fuselage and complete frame of the rocket bomber at $V/a = 1.5$ and 3, can be computed. From the Figs. we read off the best reciprocal glide number $1/\epsilon = 3.94$ for $V/a = 1.5$ and $\alpha \doteq 8°$ and $1/\epsilon = 3.83$ for $V/a = 3$ and $\alpha \doteq 7°$. Wind tunnel measurements of the polars, which are feasible in this domain, could not be carried out. In the calculation a total vacuum was assumed behind the stubby stern-surfaces. Actually these surfaces, in this velocity range where the motor is off and they are not in contact with the flame, can be acted on by oticeable pressures which make the wind resistance appear to be less than when the motor is going; this must also be noted for wind-tunnel measurements.

For $V/a \to \infty$ the thermal velocities of the air molecules and the pressure of the undisturbed air are respectively negligible compared to the flight speed and the dynamic pressure on the surfaces struck by the air stream. The part of this normal pressure p_i which arises from molecules bouncing into the wall can be taken directly from Newton's law for inelastic collisions: $p_i/q = 2 \sin^2\alpha$ Whether there is a further contribution to the pressure depends on how these molecules leave the surface. For dense air this must take place along the surface of the plate. If the wall were flat and the density of the gas layer which streams away were infinite, then the air molecules coming off would receive no acceleration perpendicular to the plate and there would be no further pressure contribution. According to V. Karman the ratio of density increase $\Delta \rho$ to density ρ before collision is $\Delta\rho/\rho = 2/(\varkappa-1)$ when the corresponding air pressure ratio is $\Delta p/p = \infty$, so this case can occur only for $\varkappa = 1$. For $\varkappa = 1.4$, $\Delta\rho/\rho = 5$, the air density at the plate is 6 times as large as for still air, the layer has a finite thickness, the angle of impact of the air is greater than the angle of attack, and the air pressure p is greater than p'; according to Busemann $p/q = (\varkappa +1)\sin^2\alpha$. As far as the value of $\varkappa$ is concerned, the molecular collisions in the flow of the condensations are sufficient in number to fully excite all molecular rotations; i.e., $\varkappa = 1.4$. If the high stagnation temperatures necessary for
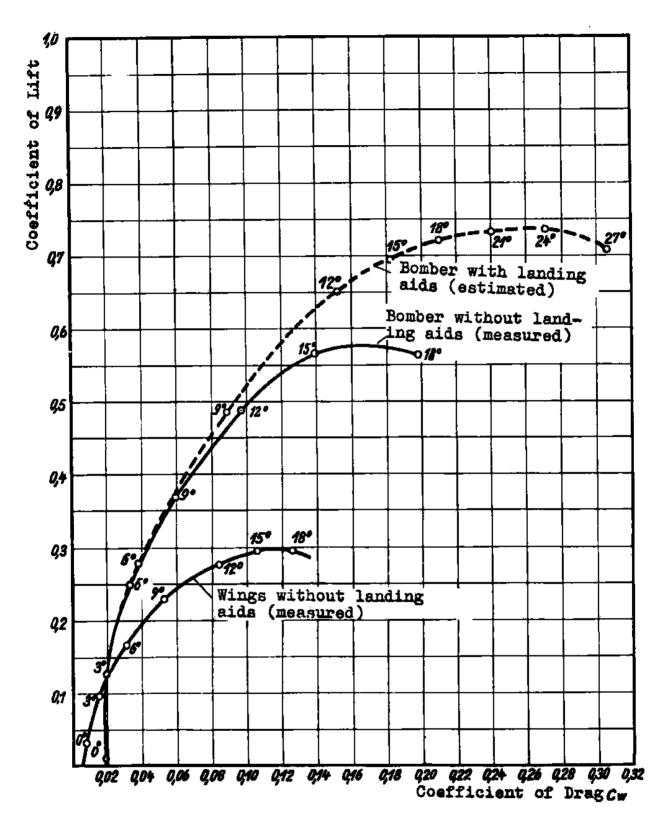
58

Figure 34;   Wind tunnel measurements at Reynolds' Number 4x10^6 and Mach number corresponding to the landing speed. (The aerodynamic coefficients are based on the area of the supporting surfaces.)
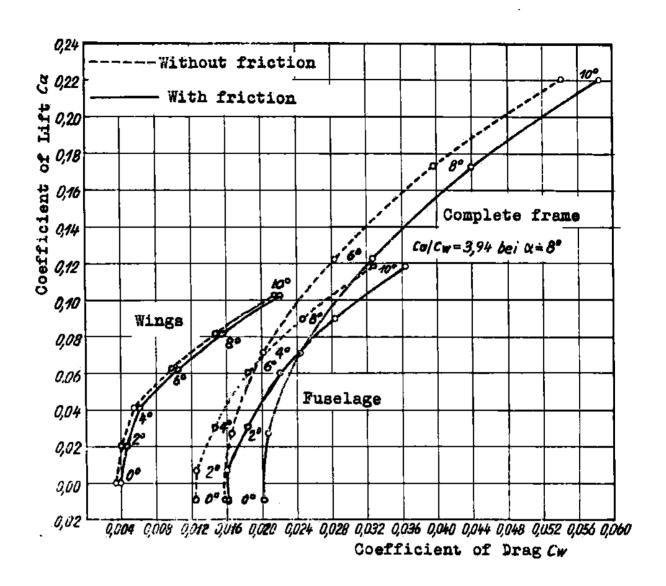
Figure 35; Calculated polars of wings, fuselage, and of the entire frame of the Rocket Bomber in the gas dynamic region and M = 1.5. These aerodynamic values are based on the area of the supporting surfaces.